GEOLOGICA CARPATHICA, AUGUST 2021, 72, 4, 344–357 https://doi.org/10.31577/GeolCarp.72.4.5

The ^{40}Ar–^{39}Ar dating and geochemistry of the Carpathian C1 obsidians (Zemplín, Slovakia)

MILAN KOHÚT[1,✉], SARAH C. SHERLOCK[2] and ALISON M. HALTON[2]

[1]Earth Science Institute, Slovak Academy of Sciences, Dúbravská cesta 9, 840 05 Bratislava, Slovakia; ✉milan.kohut@savba.sk
[2]Faculty of Science, Technology, Engineering and Mathematics, The Open University Walton Hall, United Kingdom

(Manuscript received April 15, 2021; accepted in revised form July 2, 2021; Associate Editor: Lukáš Krmíček)

Abstract: In situ ^{40}Ar–^{39}Ar UV laser ablation dating of the Carpathian *C1* obsidians from the Slovakian part of the Zemplín–Tokaj area yielded new ^{40}Ar–^{39}Ar obsidian glass ages that fall in a narrow time interval of 12.07±0.37 to 11.44±0.39 Ma. This indicate that most of the Zemplín obsidian findings come from one short-time monogenic volcano, forming part of a long-lasting volcanism over the 15–10 Ma period. Chemical compositions of the Carpathian *C1* obsidians clearly indicate common similarities between all examined localities (Brehov, Cejkov, Hraň, and Viničky). Geochemically, these obsidians belong to the silica-rich, peraluminous, high-potassium, calc-alkaline rhyolite series volcanic rocks of ferroan character. They were derived by multi-stage magmatic processes, from mixed mantle and crustal sources, and generated during subduction in a volcanic arc tectonic setting. The primary basaltic magma formed from the melting of the lower crustal source at the mantle/crust boundary. Subsequent formation of melt reservoirs in the middle and upper crust, accompanied by secondary melting of the surrounding rocks with continual addition of ascending melt, and repeated processes of assimilation and fractionation produced rhyolitic rocks with obsidians in the Zemplínske vrchy Mts.

Keywords: obsidian, ^{40}Ar–^{39}Ar dating, geochemistry, genesis, Western Carpathians.

Introduction

Obsidian is instantaneously solidified (quenched) volcanic rock, originating from an acid rhyolitic melt, and is often referred to as "*natural volcanic glass*" with typical glassy lustre and usually dark jet-black, grey or brown colour. Because of its properties, such as hardness, brittleness, and/or fracture predictability, and exceptional cutting-edge quality it was an important raw material extracted and processed to produce blades, razors, knives and weapons in the past. Obsidian was widely used for tool-making (stone industry) during prehistoric times, and played a significant role in the evolution of Humankind and civilization. Volcanic glass was geologically known since the end of the 18th Century on the studied territory, and later it was documented in terms of archaeology during the 19th Century in the Zemplín–Tokaj area (on the both sides of present boundary between SE Slovakia and NE Hungary), the only natural volcanic glass region in Central Europe (see review Biró 2006). The Carpathian obsidians have been traded since the Aurignacien 28,000 yrs BP. Archaeologists have increased understanding of these rocks through geochemical provenance studies (Williams-Thorpe et al. 1984; Oddone et al. 1999; Bigazzi et al. 2000; Rosania et al. 2008). The differences in chemical compositions enabled them to designate the following Carpathian obsidian groups: ***Carpathians 1*** (***C1***) represent samples from the localities Cejkov, Malá Bara, Malá Tŕňa, Streda nad Bodrogom and Viničky (the Zemplínske vrchy Mts. – SE Slovakia, focus of this study); samples from the Tokaj Mts. of NE Hungary were designated as ***Carpathians 2*** (***C2***) comprising the localities Bodrogkeresztúr, Csepegő Forrás, Erdőbénye, Mád, Olaszliszka and Tolcsva, while obsidians from the Zakarpattia region – W Ukraine were marked as ***Carpathians 3*** (***C3***) comprising the localities Malyj Rakovets and Rokosovo.

Generally, obsidian is dominated by amorphous, dark (opaque±locally translucent) volcanic glass (≥90 volume %), with various fine-grained accessory minerals, that are observable mainly under a microscope, and reflect their embryonic crystallization from a melt. Although obsidians largely reflect the composition of the original rhyolite magma, strikingly, these fresh (unweathered) volcanic glasses, found amongst the rhyolitic/andesitic rocks in the Eastern Slovakia, have not been of interest to geologists in the last fifty years. They have been more focussed on the obsidian's rhyolitic host than its glass form through basic geological mapping, rhyolite lithology and petrography. Works focused on their genesis and the melting processes from the source, as well as the age of magmatism/volcanism and their final cooling (e.g., Slávik 1968; Baňacký et al. 1989; Kaličiak & Žec 1995; Lexa & Kaličiak 2000; Pécskay et al. 2006). The similarity in petrogenesis of the ***C1*** obsidian composition to the surrounding rhyolitic rocks was presented by Konečný (2010). The age of obsidians from the Zemplín–Tokaj area was interpreted mostly on the basis of host rocks ages – rhyolites and rhyodacites. The K–Ar biotite and whole rocks ages yielded a broad age range from 16.2±2.0 Ma to 10.6±2.0 Ma (Bagdasarjan et al. 1968, 1971; Vass et al. 1971, 1978; for the Slovakian side) and (Balogh & Rakovics 1976; Balogh et al. 1983; as well as Pécskay et al. 1986; for the Hungarian side). However, direct obsidian dating by means of uranium "Fission Tracks" method

(FT) indicated that two age groups of obsidians were present: age intervals from 17.83±1.13 to 13.71±0.82 Ma for those of the Zemplín area, and from 16.63±1.35 to 12.15±0.73 Ma, respectively from 10.38±0.77 to 8.58±0.48 Ma for those of the Tokaj area (Bigazzi et al. 1990). Recently, the studied obsidians were also dated by K–Ar method performed on whole rock samples, yielding ages from 14.95±0.65 to 14.32 ±0.58 Ma for an "*older unit*" from southern area close Streda nad Bodrogom, and "*younger unit*" in northern area between Viničky, Cejkov and Brehov showing ages from 13.52±0.81 to 11.04±0.34 Ma (Bačo et al. 2017).

The aim of this study is to provide new ^{40}Ar–^{39}Ar ages and geochemical characteristics of the ***C1*** obsidian samples from the Zemplínske vrchy Mts. with a discussion on the age of volcanic activity and origin of the obsidians (or rhyolitic rocks generally) in the study area.

Geological setting

The Carpathian obsidians of the Zemplín area belong to the Eastern Slovakian Neovolcanic Field (ESNF) in SE Slovakia where isolated Sarmatian volcanoes penetrate Miocene strata and pre-Cenozoic basement (Figs. 1, 2). The geological setting of the Zemplínske vrchy Mts. (ZVM) and their surroundings is complicated because it includes rocks from the Paleozoic to the Holocene. The ZVM forms a typical tectonic horst within the East Slovakian Basin and hosts several elevated volcanic bodies (Figs. 1b, 2). The present architecture is a consequence of back-arc extension that is associated with asthenosphere updoming and is accompanied by calc-alkaline volcanism associated with pull-apart opening during the Miocene. These events are followed by a Pannonian to Quaternary late stage regional uplift and erosion (Baňacký et al. 1989; Vass et al. 1991; Lexa & Kaličiak 2000; Pécskay et al. 2006). The pre-Cenozoic basement belongs the so-called Zemplinicum, a tectonic unit of the Central Western Carpathians (CWC), that was amalgamated into a block during youngest Neogene times in the study area. It consists of a Variscan crystalline basement (Carboniferous to Permian in age) and its Mesozoic cover. The Paleozoic basement rock sequences encompass various sedimentary and volcanic rocks, the former being cyclic and rhythmically bedded fluvial and fluvio–lacustrine sediments. Grey conglomerates, sandstones and shales, calcareous shales, grey limestones, and locally thin black coal seams are interbedded in places with acidic volcaniclastic material (Kobulský et al. 2014). However, the high-grade metamorphic rocks such as the muscovite-gneisses, biotite–amphibole gneisses, amphibolites, and metagranites that were described by Faryad & Vozárová (1997) in the vicinity of Byšta village (western of Fig. 1 b area) can be expected at deeper levels (over 2000 metres) in the cross section of Fig. 2.

The Zemplinicum's Mesozoic cover comprises conglomerates, quartzose sandstones, limestones, dolomites, and shales with gypsum all of which originated in a shallow marine environment (Kobulský et al. 2014). The ZVM territory was then weathered, eroded and peneplaned before sedimentation of Neogene strata.

The oldest Cenozoic sediments in the East Slovakian Basin are dark claystones with interbeds of sandstones, present only at depth (outside the study area). They are attributed to the Lower Miocene – Karpatian. The Lower Badenian consists of basal conglomerates, and mainly of the sandstones with the interbeds of siltstones, and grey calcareous claystones. The Middle Badenian is dominated by calcareous claystones and siltstones with thin intercalations of fine-grained sandstones and redeposited acid tuffs and tuffites, some interbeds of conglomerates and sandstones are common at the margin of ZVM. The higher parts of the formation are made of siltstones and claystones with thin interbeds of tuffitic claystones and acid tuffs. These sediments were deposited in coastal to deeper marine environments. The volcanic activity in this area started in the Upper Badenian by rhyodacite tuffs, extrusions and lava flows. The Lower Sarmatian pyroxene andesites form buried stratovolcano, hyaloclastite andesite breccia, and lava flows with their volcaniclastics – tuffs, tuffites, which were followed by bentonized rhyodacite tuffs. The Lower – Middle Sarmatian volcaniclastics were deposited subhorizontally and consist of alternating beds of rhyolite tuffs and tuffites with intercalations of clays and fine-sandy claystones. The Middle Sarmatian volcanics are formed by extrusion of coarse-porphyric rhyodacite, epiclastic rhyolite breccia with interbeds of redeposited pyroclastics. Rhyolite extrusions that transition into lava flow in the surroundings of Viničky are mainly of pyroclastic type on the southern side of the Borsuk extrusive body (Figs. 1b, 2). Epiclastic rocks contain rhyolite fragments of the Viničky body type, as well as perlites and obsidians. The Middle–Upper Sarmatian formation is characterised by calcareous clays, silts with interbeds of the acid and intermediate tuffs, tuffites, bentonites and lignite seams. The Upper Sarmatian formation consists of calcareous sands and sandstones with interbeds of calcareous clays, tuffitic clays and tuffites that were deposited in the brackish environment. The Pannonian sedimentary formation, deposited in a freshwater lacustrine and river environment, is made up of clays, silts with interbeds of sands, river gravels (Baňacký et al. 1989; Vass et al. 1991; Kobulský et al. 2014). Generally, obsidian findings in Eastern Slovakia are divided into: a) primary – autochthonous, in magmatic rhyolite extrusive rocks e.g., Viničky, Malá Bara, and volcaniclastic tuffitic rocks in Streda nad Bodrogom; b) secondary – allochtonous, in naturally displaced Quaternary accumulations as at Brehov and Cejkov; and/or c) archaeological – human-relocated obsidian occurrences within the Paleolithic/Neolithic localities and workshop sites as Hraň, Kašov, Malá Tŕňa, Cejkov, and Zemplín (Bačo et al. 2017). Due to better characterization of obsidians from the Zemplín area, representative samples for geochemistry and Ar–Ar dating were chosen from the following localities: Viničky (primary – autochthonous from the extrusive dome/flow Borsuk), Brehov, Cejkov (secondary – allochthonous) and Hraň (human-relocated).

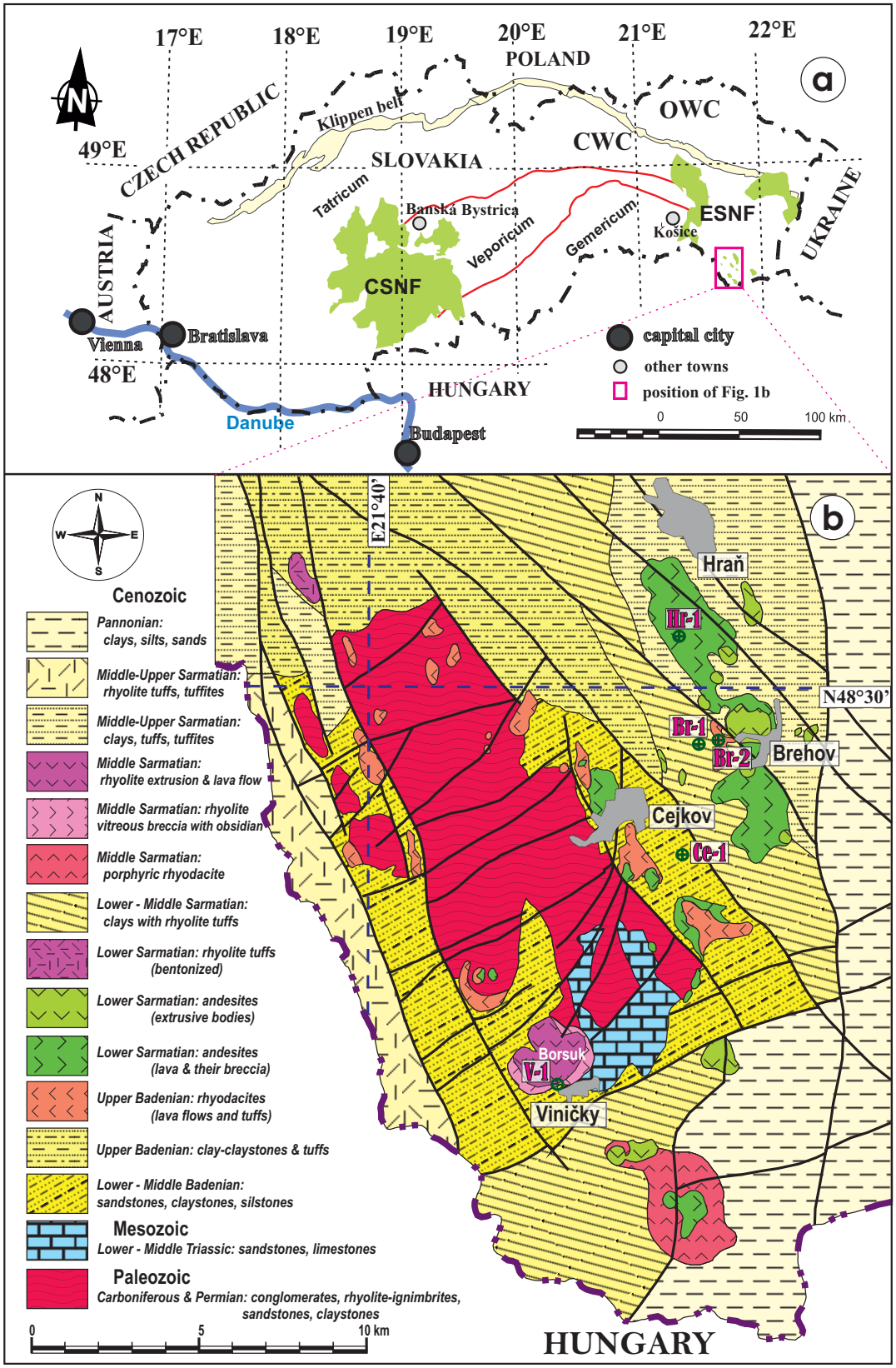

Fig. 1. Simplified geological maps and positions of studied samples. **a** — Position of the ESNF and study area within the Western Carpathians in Slovakia. *Abbreviations*: CWC – the Central Western Carpathians, OWC – the Outer Western Carpathians, CSNF – the Central Slovakians Neovolcanic Field, ESNF – the Eastern Slovakian Neovolcanic Field; Red lines denote tectonic lines dividing three principal tectonic units (Tatricum, Veporicum and Gemericum) in the CWC. **b** — Simplified and modified geological map of the ZVM based on the published map by Baňacký et al. (1989).

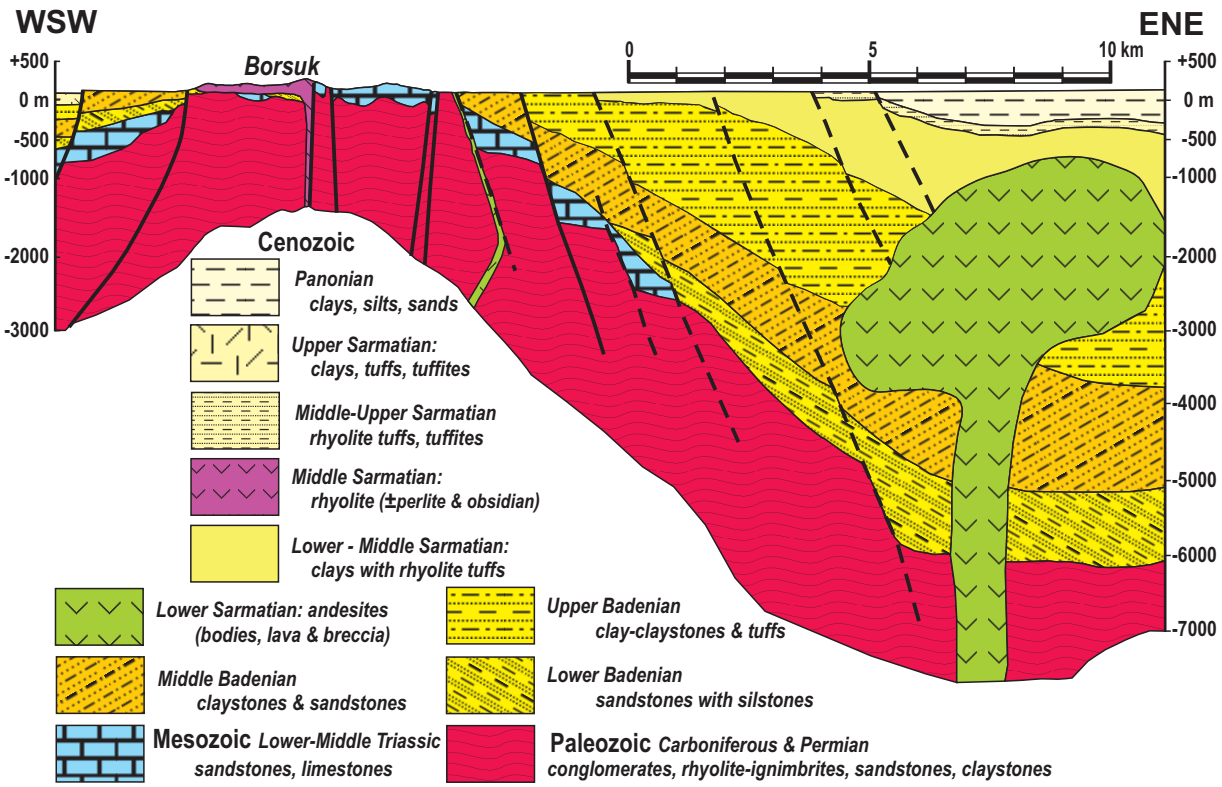

Fig. 2. Idealized geological profile through the Zemplínske vrchy Mts. and neighbouring the East Slovakian Basin, across the Borsuk volcanic body in NE–SW direction. Inspired by cross-sections published in Vass et al. (1991), and Kobulský et al. (2014).

Analytical methods

^{40}Ar–^{39}Ar dating

Sample preparation: For in-situ analysis of the obsidian samples, 150 µm thick polished sections of each sample were made and polished using 0.3 µm aluminium oxide paste. Sections were then cut to sizes appropriate for irradiation and analysis. The polished sections were cleaned ultrasonically in acetone and de-ionised water, dried using on a hot plate, and packaged in aluminium foil packets of ca. 10 mm×10 mm in size prior to irradiation.

Irradiation: Samples were irradiated at the McMaster Nuclear Reactor (McMaster University, Canada) for 4 hours. Cadmium shielding was used and the samples were held in position 8D. Neutron flux was monitored using biotite mineral standard GA1550 which has an age of 99.738±0.104 Ma (Renne et al. 2011). Standards were packed for irradiation at either side of the unknown samples and analysed using the single grain fusion method using a 1059 nm CSI fibre laser and a MAP215-50 mass spectrometer. The J values were then calculated by linear extrapolation between the 2 measured J values and the error calculated at 0.5 %.

Analysis: The irradiated samples were loaded into an ultra-high vacuum system and mounted on a New Wave Research UP-213 stage. A 1059 nm CSI fibre laser was focussed into the sample chamber with polished obsidian sections, and 50 µm diameter "in situ" spots were melted using an infra-red laser. After passing through a liquid nitrogen trap, extracted gases were cleaned for 5 minutes using two SAES AP-10 getters running at 450 °C and room temperature, following which the gases were let into a MAP 215-50 mass spectrometer for measurement, the mass discrimination value was measured at 283 for $^{40}Ar/^{36}Ar$ (using a calibration noble gas mixture of known composition). System blanks were measured before and after every one or two sample analyses. Gas clean-up and inlet is fully automated, with measurement of ^{40}Ar, ^{39}Ar, ^{38}Ar, ^{37}Ar, and ^{36}Ar, each for ten scans, and the final measurements are extrapolations back to the inlet time.

Data reduction The system blanks measured before and after every one or two sample analysis were subtracted from the raw sample data. Results were corrected ^{37}Ar and ^{39}Ar decay, and neutron-induced interference reactions. The following correction factors were used based on analyses of Ca and K salts:

$$(^{39}Ar/^{37}Ar)_{Ca}=0.00065\pm0.00000325$$
$$(^{36}Ar/^{37}Ar)_{Ca}=0.000265\pm0.000001325$$
$$(^{40}Ar/^{39}Ar)_{K}=0.0085\pm0.0000425$$

Ages were calculated using the atmospheric $^{40}Ar/^{36}Ar$ ratio of 298.56 (Lee et al. 2006) and decay constants of Renne et al. (2011). All data corrections were carried out using an Excel

macro and ages were calculated using Isoplot 3 (Ludwig 2003). All ages are reported at the 2σ level and include a 0.5 % error on the J value.

Major, trace and rare earth elements analyses

The rock samples have been analysed for whole rock chemical compositions by Bureau Veritas Commodities Canada Ltd. (former ACME Analytical Laboratories Ltd., Vancouver, BC, Canada). The multi-element lithogeochemistry of pulp samples have been performed by a lithium metaborate/tetraborate fusion and dilute nitric digestion, major elements were determined by X-ray fluorescence (XRF)/inductively coupled plasma atomic emission spectrometry (ICP–AES), trace and rare earth elements (REE) by inductively coupled plasma mass spectrometry (ICP–MS). The analytical accuracy was controlled using geological standard materials and is estimated to be within a 0.01 % error (1σ, relative) for major elements, and within a 0.1–0.5 ppm error range (1σ, relative) for trace elements and 0.01–0.05 ppm for REE.

Results

Mineralogy and petrography

Obsidian is commonly referred to as an amorphous, glassy, aphyric and chemically homogenous rock, though the accuracy of this description depends on the scale of the view and the strictness of the study. Detailed petrological study by polarizing microscopy, electron micro-probe analysis (EMPA) and micro-computer tomography (μCT) reveals that, besides comprising glass with a hyaline – vitritic structure, there is a wealth of various mineral forms, and vesicles or voids (Fig. 3a–f). The Carpathian obsidians studied here consist of a broad association of accessory minerals like plagioclase, biotite, alkali feldspar, quartz, pyroxenes, amphiboles, magnetite, Fe–Ti oxides, pyrrhotite, pyrite, chalcopyrite, olivine, zircon, apatite, monazite, uraninite, ilmenite, hercynite and garnet (Kohút et al. 2018). These minerals can be present in the form of phenocrysts (having size 100–1000 μm, Fig. 3b,f), microlites (10–50 μm, Fig. 3b,f), and hair like trichites (Fig. 3c,d). The parallel alternation of pale and dark stripes, comprising ultra-fine microlites and trichites and forming a banded texture, were the result of melt flow. Besides the autolithic origin of crystallized minerals, sporadic xenoliths from the source and/or assimilated rocks can be present. Although the majority of these minerals have the primary magmatic origin, not all of them reflect their direct crystallization from a parent rhyolite melt. Most of the plagioclases (Pl) are subhedral microlites, although there are phenocrysts of up to 450 μm present locally. Generally, these are zoned with broad chemical composition (andesine–bytownite) in the cores, whereas more acid oligoclase, and scarcely albite, compositions were identified in the rime. K-fs grains are less frequent than Pl, and sporadic anhedral grains of up to 100 μm are mainly anorthoclases, while high-temperature sanidine is also present. Biotites are mainly larger laths 100–850 μm in size, and/or smaller oval/anhedral flakes having brown pleochroic colour (Fig. 3b,f). Pyroxenes are euhedral and subhedral microlites and trichites (Fig. 3d), and locally anhedral grains in aggregates. Amphiboles were identified as subhedral microlites, and/or anhedral grains in aggregates. Magnetite are mostly small anhedral grains and trichites, and/or subhedral/anhedral xenocrystic grains of up to 45 μm, and in a few cases with typical ilmenite lamellas. Of note, the trichites have hairy shapes that when magnified up to 500× look like continuous linear alignments (5–10 μm in diameter). These are actually discontinuous, triaxial, hieroglyphic formations, documenting the rapid quenching of the flowing melt in nano dimension. Olivines were found locally with pyroxene in xenocrystic aggregates as anhedral grains 5–100 μm. Zircons form euhedral quadrate and prismatic grains 10–50 μm whilst apatites form mainly euhedral and subhedral prismatic microlites of 20–55 μm. Monazites were commonly found as subhedral grains 15–100 μm in size and/or oval grains with signs of magmatic corrosion. Ilmenite forms sporadic euhedral and subhedral grains up to 20–35 μm, and fine lamellas in magnetite. Sulphides are present as rare solitary striped mineral forms. The hercynite and garnet were found only once as small isometric corroded grains probably representing restite from source and/or assimilated host rocks.

^{40}Ar–^{39}Ar data

The Ar–Ar data from 4 dated glass samples (Br-1, Br-2, Ce-1 and V-1), and biotite phenocrysts from Br-2 and Ce-1 are shown in Supplementary Table S1. Ten to twenty "in situ" spot measurements from each glass sample, and five to ten spots analysis on the 3–6 different biotite phenocrysts from Br-2, Ce-1 samples were realized. The measurements with big error (due to very small gas volume) or meaningless ^{36}Ar contents were excluded from age calculations. Weighted mean ages for analysed glass and biotite samples are reported at the 2σ level in Fig. 4. Four analysed obsidian glass samples date an interval of rhyolitic volcanism in the ZVM area at 12.07±0.37 to 11.44±0.39 Ma. These ages fall within the 16.2–10.6 Ma interval of known K–Ar ages from the rhyolite and rhyodacite host rocks from the Eastern Slovakia (Bagdasarjan et al. 1968, 1971; Vass et al. 1971, 1978; and review in Pécskay et al. 2006). Similarly, they overlap with the youngest recently published obsidian K–Ar whole rocks ages, e.g. 14.7–11.0 Ma (Bačo et al. 2017). However, our Ar–Ar data are younger than published FT ages (17.8–13.7 Ma) from the Zemplín area (Bigazzi et al. 1990). On the other hand, our ages compare well with recently published 12.45±0.40 to 11.62±0.25 Ma FT ages (Kohút et al. 2021), from identical localities, and suggest a considerably tighter age interval of rhyolitic volcanism in the Zemplín region compared to the ages that were previously presented 15–10 Ma (see review Pécskay et al. 2006; Bačo et al. 2017). Further, the ages presented in this study are comparable to recent K–Ar ages of the rhyolitic volcanic rocks

from the Telkibánya lava domes (Tokaj Mountains) that have intrusion ages of 11.56±0.15 to 11.47±0.19 Ma (Szepesi et al. 2019). However, two Ar–Ar weighted mean ages of 14.5±2.1 and 12.4±1.0 Ma for biotites in this study indicate a longer interval, reflecting crystallization processes in a magma chamber (Fig. 4e, f). Anyway, the older ages come

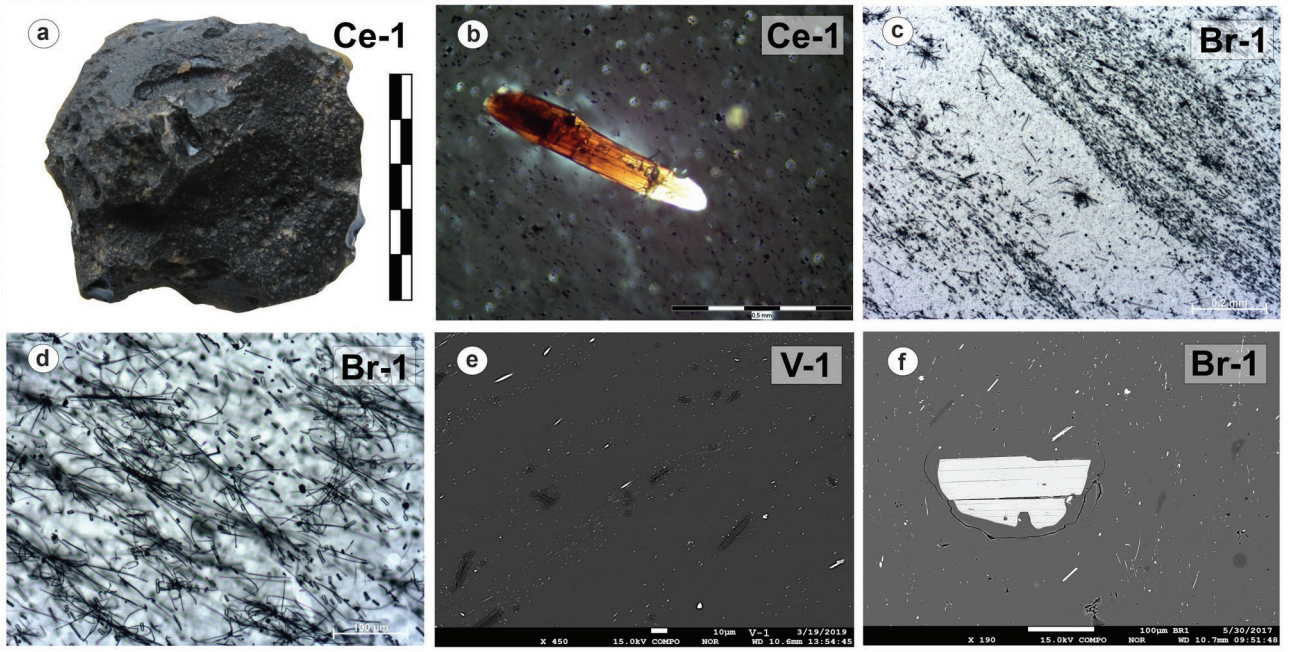

Fig. 3. Macro and micro views of the studied obsidian samples: **a** — typical shape of obsidian from the Cejkov-1 (Ce-1) locality, scale bar 5 cm; **b** — large phenocryst of biotite in sample Ce-1, polarized light (crossed nicols) in polarised microscope; **c** — banded texture in sample Br-1, plane light (parallel nicols); **d** — trichites and fine microlites in sample Br-1, plane light (parallel nicols); **e** — fine-grained linear and banded alignments of trichites in sample V-1, back scattered electrons image (BSEI) from electron micro probe (EMP); **f** — phenocryst of biotite in sample Br-1, BSEI.

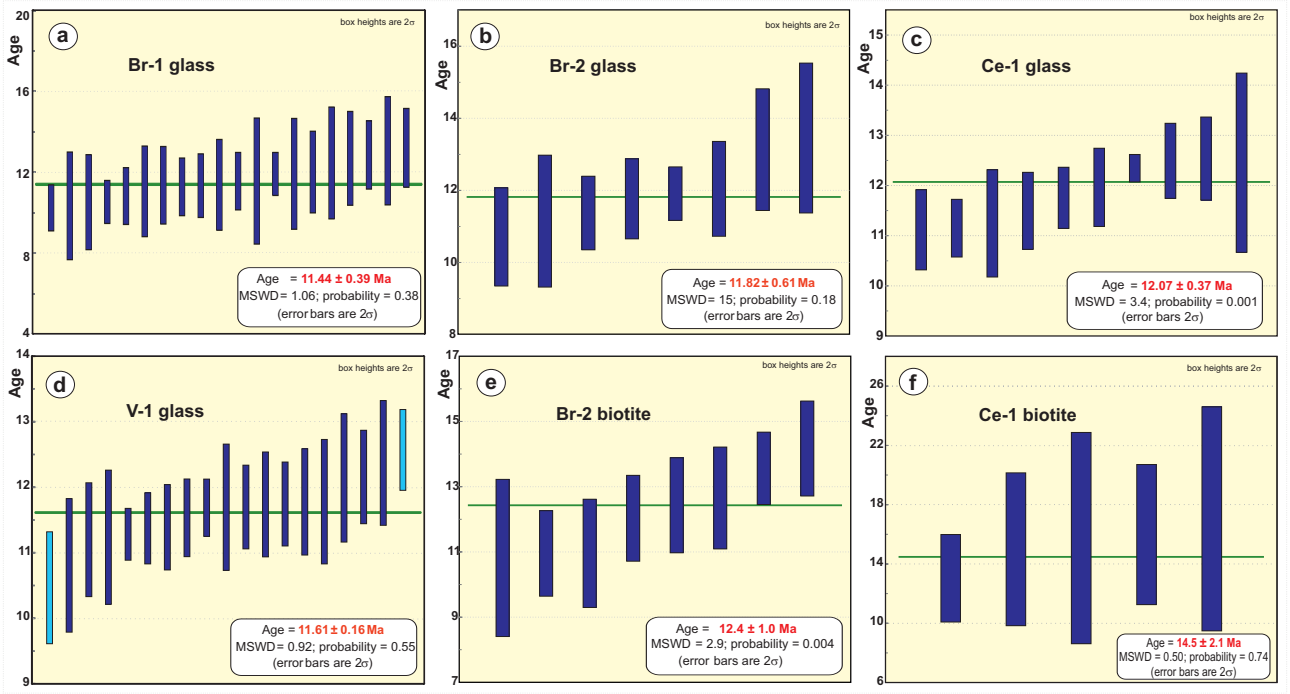

Fig. 4. $^{40}Ar/^{39}Ar$ results for the analysed ***C1*** obsidian samples; weighted mean ages (reported with 2σ uncertainties). The light blue colour analyses (Fig. 4d) were excluded from weighted mean age 11.61±0.16 Ma, because they "don't touch" this referred age line with its error propagation, although the age calculated with these two analyses is similarly good 11.68±0.31 Ma.

from antecrystic biotites that exhibit frequent magmatic corrosion.

Chemical composition of obsidians

New WR chemical analyses on the Carpathian ***C1*** obsidian samples are given in Table 1. Notably, archaeologists have analysed only an eclectic set of elements (often missing some important petrogenetic elements) in their provenance studies; therefore these data are not suitable for petrochemical genetic interpretations. Major-element analyses of the ***C1*** obsidians have been published by Šalát & Ončáková (1964), Kaminská & Ďuďa (1985) but these data are incomplete and not considered in this study. A small number of complete data ***C1*** obsidians were published by Rózsa et al. (2006), and by Illášová & Spišiak (2011). Weighted means of the 6–7 spot measurements from EMPA and LA ICP MS analysis (Kohút et al. 2021) strictly representing the composition of glass from the studied obsidians are presented here for comparison. In addition some representative analyses of the host rocks of the ZVM (Konečný 2010) are compared with our obsidian analyses.

Table 1: Chemical composition of the Carpathian ***C1*** obsidians from the Zemplín area, Slovakia. Major elements in wt. %; minor elements in ppm; Au in ppb. Sample ObV-1 is taken from Illášová & Spišiak (2011), and V-8 from Rózsa et al. (2006).

Sample	Br-1a	Br-1b	Br-2a	Br-2b	Ce-1a	Ce-1b	Ce-1c	Hr-1a	Hr-1b	V-1a	V-1b	ObV-1	V-8
SiO_2	76.33	75.95	76.31	75.61	75.84	75.64	75.72	76.39	75.72	76.13	76.25	76.15	76.36
TiO_2	0.05	0.06	0.05	0.06	0.06	0.05	0.05	0.05	0.05	0.06	0.06	0.07	0.06
Al_2O_3	12.87	12.89	12.81	13.04	12.92	13.08	13.04	12.77	12.83	12.78	13.05	13.14	13.22
FeO^t	1.01	1.16	1.01	1.05	1.05	1.10	1.09	1.07	1.09	1.04	1.08	1.19	1.19
MnO	0.05	0.04	0.05	0.05	0.06	0.05	0.05	0.05	0.04	0.05	0.05	0.05	0.04
MgO	0.08	0.10	0.08	0.07	0.11	0.07	0.07	0.09	0.08	0.10	0.09	0.11	0.06
CaO	0.79	0.87	0.82	0.85	0.88	0.93	0.91	0.85	0.88	0.88	0.94	0.97	0.95
Na_2O	3.48	3.43	3.46	3.61	3.59	3.53	3.47	3.42	3.73	3.45	3.46	3.39	3.48
K_2O	4.52	4.49	4.43	4.57	4.53	4.54	4.56	4.38	4.55	4.45	4.35	4.38	4.08
P_2O_5	0.02	0.02	0.02	0.03	0.02	0.03	0.03	0.02	0.03	0.02	0.03	0.03	0.04
LOI	0.46	0.54	0.59	0.60	0.55	0.54	0.53	0.55	0.64	0.63	0.49	0.40	0.44
Total	99.66	99.55	99.63	99.54	99.61	99.56	99.52	99.64	99.64	99.59	99.85	99.88	99.92
Ba	388	511	436	456	468	487	484	468	490	468	489	532	487
Sc	3.4	2.0	3.5	2.0	3.6	2.0	2.0	3.6	2.0	3.6	3.2	3.0	2.0
Be	5	3	2	3	4	4	4	3	4	2	3	4	3
Co	0.4	0.8	0.6	0.5	0.3	0.5	0.6	0.8	0.6	0.4	0.6	0.7	0.6
Cs	11.2	9.6	10.3	11.0	9.5	10.2	10.2	9.7	10.0	9.0	9.5	9.8	9.6
Ga	13.5	13.8	13.2	13.8	12.1	14.4	13.3	12.7	14.0	13.6	14.4	15.2	14.3
Hf	2.6	2.8	2.5	2.6	2.5	2.6	2.6	2.5	2.7	2.3	2.5	2.8	2.4
Nb	8.3	8.8	8.2	9.1	8.1	9.1	8.5	8.0	8.9	7.6	8.7	9.1	9.8
Rb	183.7	171.8	177.9	183.9	166.5	179.1	171.2	168.3	173.5	168.4	176.5	190.4	179.0
Sr	53.2	75.4	57.4	60.5	65.9	67.4	65.7	61.0	70.0	65.5	74.2	85.1	75.0
Ta	1.5	1.3	1.3	1.4	1.3	1.5	1.4	1.4	1.4	1.2	1.5	1.4	1.7
Th	14.7	18.5	15.9	17.2	16.3	17.2	17.2	16.2	17.8	16.2	16.5	16.8	16.0
U	9.9	8.7	9.7	10.0	9.2	8.6	9.1	8.8	9.2	8.8	8.7	8.5	8.5
Zr	59.7	72.0	62.8	68.1	63.1	69.8	68.8	63.3	71.4	63.5	65.6	70.6	62.0
Y	30.0	28.0	27.9	30.0	28.3	29.2	27.8	26.8	28.9	26.6	26.8	27.1	23.0
La	23.70	31.10	26.10	27.30	27.50	29.20	29.30	26.70	29.40	28.00	27.60	28.20	24.20
Ce	45.10	58.50	50.00	53.20	51.30	57.40	56.30	50.80	57.70	55.00	56.50	58.90	49.10
Pr	5.08	6.71	5.56	6.03	5.87	6.38	6.37	5.71	6.50	5.97	6.12	6.24	6.10
Nd	17.60	22.70	19.60	21.50	20.80	21.60	22.20	19.30	22.50	21.20	21.80	22.50	19.20
Sm	3.64	4.33	4.12	4.28	4.23	4.33	4.38	4.04	4.30	4.11	4.16	4.22	3.50
Eu	0.27	0.43	0.30	0.34	0.33	0.37	0.37	0.34	0.41	0.38	0.38	0.39	0.31
Gd	3.91	4.13	3.95	4.20	4.00	4.26	4.15	3.88	4.27	4.05	4.01	3.91	4.60
Tb	0.72	0.72	0.72	0.75	0.71	0.73	0.71	0.70	0.73	0.69	0.71	0.71	0.70
Dy	4.55	4.40	4.67	4.88	4.28	4.72	4.67	4.22	4.56	4.44	4.28	4.14	3.97
Ho	0.97	0.97	1.00	1.05	0.92	0.96	0.93	0.91	0.94	0.91	0.89	0.84	0.98
Er	2.96	2.77	3.07	3.00	2.72	2.93	2.97	2.82	2.90	2.85	2.75	2.59	2.83
Tm	0.47	0.43	0.45	0.46	0.42	0.43	0.44	0.43	0.42	0.42	0.42	0.41	0.45
Yb	3.17	2.71	2.95	3.04	2.75	2.99	2.94	2.78	3.00	2.76	2.78	2.80	2.26
Lu	0.46	0.43	0.47	0.46	0.45	0.44	0.45	0.44	0.44	0.44	0.42	0.41	0.42
Cu	1.6	1.7	1.5	3.2	2.2	4.2	2.9	2.3	3.8	1.2	2.3	3.2	1.8
Pb	12.3	12.2	12.1	11.8	13.5	13.1	12.4	13.2	15.1	12.1	12.4	11.4	12.9
Zn	2.0	2.0	2.0	2.0	3.0	3.0	1.0	2.0	4.0	2.0	2.5	21.0	2.7
Ni	5.8	5.6	6.6	7.8	6.3	5.2	4.4	5.6	6.4	4.7	4.5	4.1	4.3
Au	21.9	28.4	32.4	34.3	43.9	25.4	32.6	36.3	25.4	35.6	37.2	62.7	–

In terms of their geochemistry, the ZVM obsidians are typical volcanic calc-alkaline rocks (Fig. 5a–f). Their SiO_2 content varies in a narrow range from 75.6 to 76.4 wt. %, while the surrounding host rocks (rhyolites, dacites±andesites) have silica contents ranging from 65.9 to 77.4 wt. %, which reflects their evolved fractionated character. The ***C1*** obsidians have generally elevated content of potassium varying in a narrow interval (K_2O=4.08–4.57 wt. %) thus falling among the high potassium calc-alkaline igneous rocks, according to Peccerillo & Taylor (1976), whereas part of dacitic/andesitic host rocks, with lower values (2.7–3.2 wt. %) inclines to medium potassium calc-alkaline rocks (Fig. 5b). The relatively increased values of FeO^t along with decreased values of MgO in the ZVM obsidians, as well as the surrounding host rocks, indicate their general ferroan character in accordance with Frost et al. (2001) (Fig. 5d). The Aluminum Saturation Index (ASI – molar ratio $Al_2O_3/(CaO+Na_2O+K_2O)$=1.04–1.11) indicates their mildly peraluminous character and possible limited coexistence of hornblende and pyroxene with peraluminous magma, which agrees with microscope observations (Fig. 5e). The high calc-alkaline character with affinity to shoshonite series, of the studied ***C1*** obsidians, confirm contents of the minor elements as well as, namely in classical diagram of Pearce (1982) by Th/Yb vs. Ta/Yb ratios (Fig. 5f). The chemical composition of the obsidian samples, recalculated for the normative values of Q (quartz), P (plagioclase) and A (K-feldspar), support their rhyolitic composition in the classification diagram QAP of Streckeisen (1976) (Fig. 6a). The normative compositions of the host rocks show a wider compositional range from rhyolites to dacites, mirroring the prevalence of plagioclase within some samples. On the basis of the normative composition of the feldspars, the studied obsidians fall into the rhyolite field in the ternary Ab–An–Or discrimination diagram of O'Connor (1965) whereas some of the host rocks volcanics plot within the rhyodacites field. The Q'–ANOR classification diagram (Streckeisen & Le Maitre 1979), based on the improved granite Mesonorm (Mielke & Winkler 1979), provided an identical evaluation of the studied obsidians as typical rhyolites and part of the host rocks as dacites (Fig. 6b). The evolved, differentiated nature of the ZVM rhyolite/obsidian magma in combination with the homogeneous composition of the studied obsidians is well documented in the TAS diagram (Total Alkali Silica, Cox et al. 1979; Middlemost 1994) where projection points of the samples form a narrow field within the most fractionated rhyolites, while the host rocks scattered over the broad dacite–rhyolite area. A similar result was obtained using the De la Roche et al. (1980) R_1–R_2 classification scheme (Fig. 6c), in which all the obsidians define a narrow rhyolite field, and the host rocks spread from the alkali rhyolite into the rhyodacite/dacite fields. The K_2O/Na_2O ratio of the obsidians varies from 1.17 to 1.34 and this minor predominance of potassium shows that they belong to the sodium–potassium magmatic province (Niggli 1923); however, in the surrounding rhyolites and dacites this ratio is more balanced. The Rb/Sr ratios range from 2.24 to 3.45, indicating a significant degree of differentiation of these volcanic rocks, which is not so pronounced in most of the host rocks which have Rb/Sr ratios of 0.47–2.82. The trace element compositions of the ZVM obsidians are well documented in the Zr/TiO_2 vs. Nb/Y diagram, which is essentially a proxy for the TAS classification diagram, where Nb/Y is an alternative for alkalinity (Na_2O+K_2O) and Zr/TiO_2 is a proxy for silica (Pearce 1996), showing that all samples plot within the rhyolite & dacite field (Fig. 6d). Chondrite normalized REE patterns (Boynton 1984) of studied samples show uniform distribution trend with a pronounced negative Eu anomaly, Eu/Eu*=0.22–0.31, La_N/Yb_N=5.04–7.74 and partially elevated HREE values compared to the rhyolite and dacite hosts (Fig. 7a). Noteworthy, the marked difference in HREE between the whole rock analyses of the ***C1*** obsidians (this study) and glass compositions from identical samples, does not reflect contribution from identified accessory REE-rich minerals (Kohút et al. 2021), but rather point to derivation from a basaltic precursor, instead of high degrees of crustal contamination. It is suggested that this depletion is caused by the presence of pyroxene microlites and trichites (Fig. 3c,d). However, NMORB normalization (Sun & McDonough 1989) clearly indicate the crustal character of the parent magma because of it elevated LILE concentrations (Rb, Ba, K, Pb), and depletion in P and Ti (Fig. 7b).

Discussion

Dating of the C1 obsidians

In the past, the age of the ZVM – ***C1*** obsidians was mostly interpreted on the basis of the K–Ar dating results for the volcanic rhyolite and rhyodacitic host rocks. The lithostratigraphy and/or biostratigraphy of the sedimentary sequences of the surrounding East Slovakian Basin (including intercalated tuff layers) was determined by (Baňacký et al. 1989; Vass et al. 1991). However, because the Zemplínske vrchy Mts. form a tectonic horst, the correlation between the fill of the East Slovakian Basin and the ZVM is not very clear. The available biotite and rhyolite whole rock K–Ar ages define a wide age interval of 16.2±2.0 Ma to 10.6±2.0 Ma (Bagdasarjan et al. 1968, 1971; Tsoň & Slávik 1971; Vass et al. 1971, 1978). These age determinations were performed during the basic mapping study of the East Slovakian Basin on the Slovakian side of the Zemplín–Tokaj area. However, only scattered information is available from the vicinity of the obsidians studied here, including the Hrčeľ rhyolite quarry (8.5 km from Hraň, and 10 km to Cejkov) and Malá Bara rhyolite (2 km from Viničky) see Table 2. Several authors have suggested that volcanism was long-lasting, from the Langhian to the Tortonian (Badenian to Sarmatian), or occurred during two separate volcanic phases. Noteworthy, that Bačo et al. (2017) defined four age groups of obsidian on the basis of a classical K–Ar dating method: 1) Streda nad Bodrogom reworked volcaniclastic rocks with obsidian (14.95–14.32 Ma); 2) Brehov, Cejkov obsidian in allochtonous and archaeological occurrences

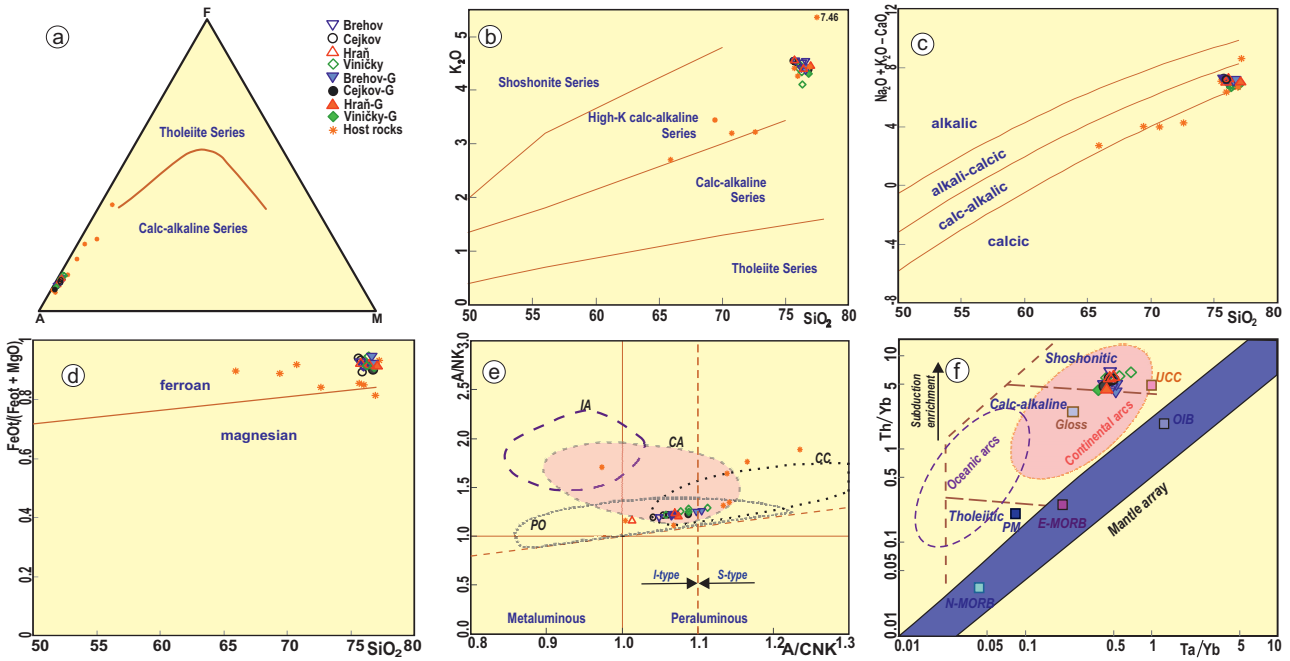

Fig. 5. Geochemical classification diagrams for the studied obsidians and their rhyolitic host rocks: **a** — AFM diagram [alkali (Na_2O+K_2O) – total iron FeO^t – magnesium MgO] after Irvine & Baragar (1971) documenting the affinity of the ZVM obsidians to the calk-alkaline rhyolitic series; **b** — K_2O vs. SiO_2 diagram (in wt. %; Peccerillo & Taylor 1976) indicating the high-potassium content of the studied samples; **c** — modified alkali-lime index (Na_2O+K_2O-CaO) against SiO_2 (all in wt. %; Frost et al. 2001) showing the calk-alkaline character of the ***C1*** obsidians; **d** — Fe-number ($FeO^t/(FeO^t+MgO)$ vs. SiO_2 (all in wt. %) diagram after Frost et al. (2001) demonstrating the ferroan nature; **e** — molar values $A/NK=Al_2O_3/(Na_2O+K_2O)$ vs. $A/ANK=Al_2O_3/(CaO+Na_2O+K_2O)$ [commonly referred to as the Aluminum Saturation Index – ASI] showing mild peraluminosity of the ZVM obsidians, abbreviations for the geo-tectonic environment fields: CC – continental collision, CA – continental arc, IA – island arc, and PO – post-orogenic are taken from Maniar & Piccoli (1989); **f** — Th/Yb versus Ta/Yb diagram (Pearce 1982) documenting the shoshonitic/highly calk-alkaline character of the ***C1*** obsidians on the basis of trace element contents; PM – primitive mantle, N-MORB+E-MORB – normal + enriched mid-ocean ridge basalts, OIB – ocean island basalts are according Sun & McDonough (1989); Gloss – **glo**bal **s**ubducted **s**ediments (Plank & Langmuir 1998); UCC – upper continental crust (Taylor & McLennan 2001).

(13.51–12.03 Ma); 3) Viničky obsidian in rhyolite lava flow (13.52–11.58 Ma); and 4) Viničky obsidian in rhyolite intrusion (11.19–11.04 Ma). Data presented in this study indicate derivation of studied geological and archaeological obsidian samples mainly from the Viničky–Borsuk rhyolite lava dome/flow, representing the younger silicic volcanics unit of the ZVM.

Biotite and rhyolite whole rock K–Ar ages for the Miocene volcanics of the Tokaj Mts. of NE Hungary more or less yielded a comparable age range from 14.6±0.8 Ma to 10.5±0.4 Ma (Balogh & Rakovics 1976; Balogh et al. 1983; Pecskay et al. 1986, 2006; Szepesi et al. 2019). Interestingly, the rhyolites from the obsidian locality Erdőbénye yielded very similar ages of 12.2±0.4 Ma and 11.5±0.5 Ma (Pecskay et al. 1986) which fit well with the obsidian FT dates (Kohút et al. 2021) and age data of this study.

It is clear that these current FT and Ar–Ar data (Kohút et al. 2021; and this study) show good compatibility of ages that fall in the narrow age interval range of 12.45±0.45 and 11.44±0.39 Ma in the frame of the younger ZVM obsidian/rhyolite magmatism unit. Due to the lack of data from the older unit (Streda nad Bodrogom area) it was not possible to confirm yet a long-lasting, multi-pulses rhyolitic volcanism spanning ca. 15–10 Ma, from the Langhian to the Tortonian (Badenian to Sarmatian) stages of the Miocene period (see review Pécskay et al. 2006; Bačo et al. 2017). This Serravallian short-time period is reflected in a general weighted mean age of 12.0±0.5 Ma, suggesting a monogenic volcanic evolution in the younger silicic volcanics unit of the ZVM, which is also supported by the identical chemical composition of the all ***C1*** obsidian samples in this study. Noteworthy, there is congruence not only in the chemical composition of the obsidians, but also in the results of a comprehensive physical study, including μCT scanning, X-ray spectroscopy, Raman spectroscopy, Mössbauer spectroscopy, positron annihilation lifetime spectroscopy (PALS), thermogravimetric analysis (DTA), Fourier-transform infrared spectroscopy (FTIR), magnetic susceptibility, including thermomagnetic properties, electron (spin) paramagnetic resonance (ESR/EPR), and SQUID magnetometry. A high degree of uniformity exists amongst these ***C1*** obsidians (Kohút et al. 2019).

Genesis of the C1 obsidians

The origin of the Neogene to Quaternary volcanic/magmatic rocks in the Carpathian–Pannonian Region is traditionally

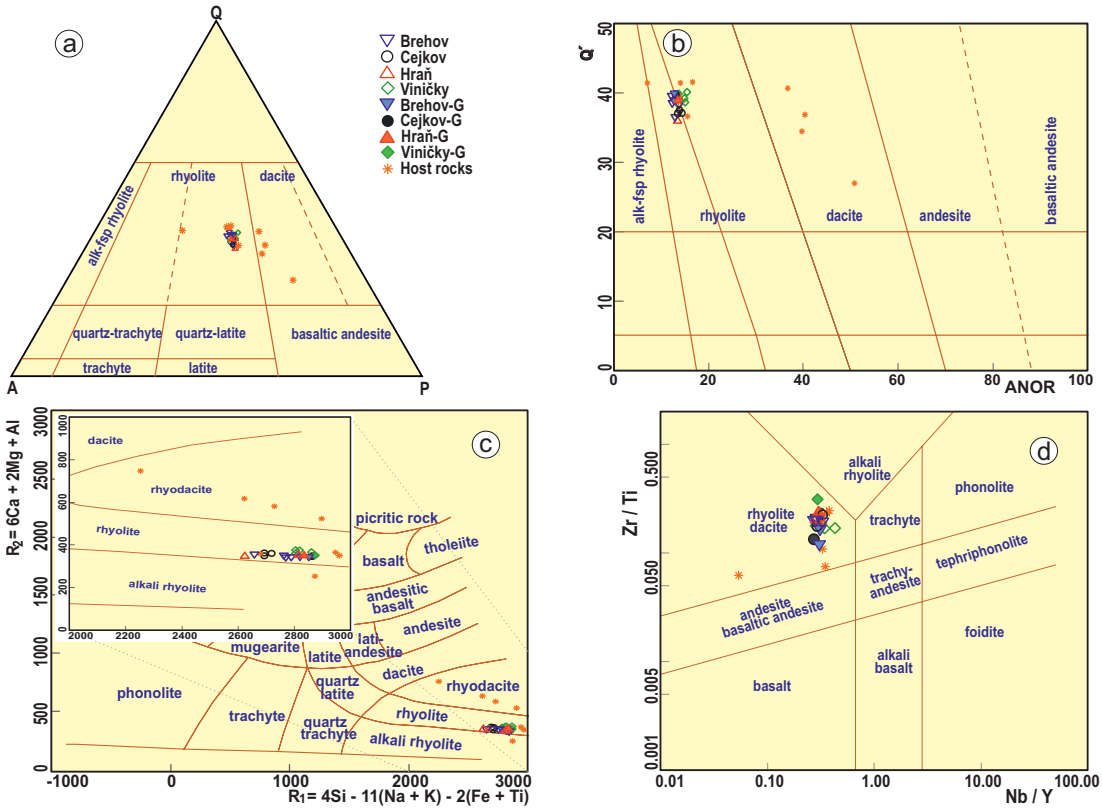

Fig. 6. Additional petrographical nomenclature and geochemical classification diagrams: **a** — the QAP classification diagram (Streckeisen 1976) based on the normative contents of quartz, alkali feldspar, plagioclase, proving the shared rhyolitic character of the ***C1*** obsidians; **b** — Q'–ANOR diagram (Streckeisen & Le Maitre 1979) based on the improved granite Mesonorm (Mielke & Winkler 1979); **c** — R_1–R_2 chemical variation diagram (De la Roche et al. 1980) showing the resemblance of the ZVM obsidian to rhyolitic rocks; **d** — Zr/TiO_2 vs. Nb/Y diagram of Pearce (1996), which is widely used as an immobile element proxy for the TAS diagram.

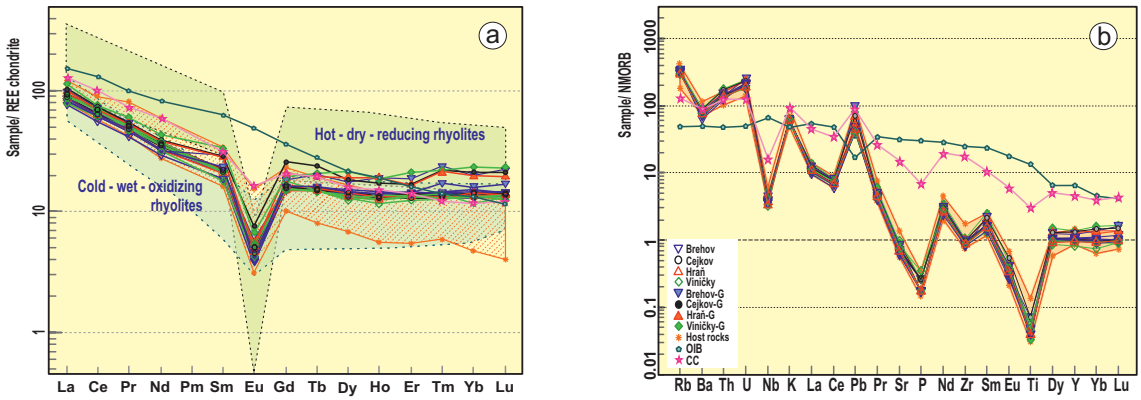

Fig. 7. Normalized REE and multi-element plots: **a** — C1 chondrite normalized (Boynton 1984) spider diagram of the ZVM obsidians and host rocks, OIB – ocean island basalt (Sun & McDonough 1989) and CC (Taylor & McLennan 2001) are shown for comparison; **b** — N-MORB normalized (Sun & McDonough 1989) incompatible trace element variations for the Carpathian ***C1*** obsidians and host rocks, the OIB and CC patterns of Fig. 7a are shown for comparison.

explained by a complex interplay of subduction with rollback, back-arc extension, collision, slab break-off, delamination, strike-slip tectonics and microplate rotations. In addition, there is the evolution of magmas in the crustal environment due to differentiation, crustal contamination, anatexis and magma mixing (Salters et al. 1988; Lexa et al. 2010; Seghedi & Downes 2011). The equivocal mineralogy of the ***C1*** obsidians suggests that they are not just ordinary crustal peraluminous melt products, since the Fe–Ti oxides (magnetite) together with Fe-pyroxene (ferrosilite), crystallized during a late magmatic stage as microlites and trichites. This corresponds to their overall ferroan character, which is not a typical feature of silicic peraluminous magmatic rocks, and is supported by the increased abundances of gold (Au=22–63 ppb

see Table 1), which is common for basaltic rocks. The chemical composition of the ***C1*** obsidians clearly suggests that they were produced in a continental arc tectonic environment (Fig. 5e, f, and Fig. 8a, b) during subduction/collision processes. The mildly peraluminous to subaluminous (ASI=ca 1.05) character of the obsidians indicate a complex (I/S-type) origin, reflecting participation of a mantle derived precursor melt and subsequent fractionation with crustal assimilation (Fig. 5e). Naturally, the basaltic precursor was extensively diluted by melt from subducted sediments (Gloss, e.g. Plank & Langmuir 1998), and sequentially by repeated fractionation and/or mixing with purely crustal melts, whereby they gained an overall silicic character at the late stage (Figs. 5f, 8b). However, one of the first geotectonic evaluations based on trace elements ratios (Bailey 1981) indicates a transition between a continental island-arc and an Andean-type volcanic arc (Fig. 8a), whereas Ta, Th, Nb and Yb concentrations (Fig. 5f, and Fig. 8b) of the ***C1*** obsidians evidently point to their generation in a continental volcanic arc according to Pearce (1996) and Saccani (2015). The ZVM obsidians are classified as a typical mixed I/S-type volcanic rock of crustal/mantle origin, which is detectible in the Na_2O vs. K_2O classification diagram where they plot on the boundary between the I/S-type mixed magmatites (Chappell & White 1992). They have correspondingly lower concentrations of iron (FeO^t=1.01–1.19 wt. %) and calcium (CaO= 0.77–0.97 wt. %), as reflected in the CaO vs. FeO^t diagram (Chappell & White 1992) where they plot into the transition I/S-type zone, albeit there is a general deficiency of the ferromagnesian minerals. All analysed ***C1*** obsidian samples plot in the evolved acidic rhyolitic field and are of sub-alkaline character, whereas part of the host rocks show an affinity to intermediate compositions. Normalized REE patterns of the studied samples show a uniform distribution trend with a pronounced negative Eu anomaly, and partially elevated HREE values compared to the rhyolite and dacite host rocks. Their chondrite normalized REE patterns fall on the boundary between "hot-dry-reduced" and "cold-wet-oxidized" magmas (Bachmann & Bergantz 2008) reflecting genesis of magma from mantle and crustal sources (Fig. 7a). The CaO/Na_2O vs. Al_2O_3/TiO_2 and Rb/Ba vs. Rb/Sr binary plots (Sylvester 1998) clearly indicate that the ZVM obsidian samples fit mixing trajectories with dominant crustal magma proportions and weak (10–30 %) contributions from a mantle component (Fig. 9). The Carpathian ***C1*** obsidians, and their rhyolite and

Table 2: Review of the existing age data from the studied area. A – authors: 1) Bačo et al. (2017); 2) Kohút et al. (2021); 3) Tsoň & Slávik (1971); 4) Bigazzi et al. (1990); 5) Vass et al. (1978); 6) Repčok et al. (1988); 7) Bagdasarjan et al. (1971); 8) Repčok (1977).

	Rhyolite			Obsidian			Obsidian			This study	
Locality	**K–Ar**	**±2σ**	**A**	**K–Ar**	**±2σ**	**A**	**FT**	**±2σ**	**A**	**Ar–Ar**	**±2σ**
Brehov	–			**12.45**	**0.95**	1	**11.62**	**0.25**	2	**11.82**	**0.61**
Brehov	–			–			–			**11.44**	**0.39**
Cejkov	14.00	1.10	3	13.48	0.72	1	16.71	1.08	4	**12.07**	**0.37**
Cejkov	14.10	2.00	3	–			16.14	1.02	4	–	
Cejkov	13.30	1.10	5	–			15.45	1.10	4	–	
Cejkov	13.40	2.00	5	–			–			–	
Cejkov	**11.50**	**1.20**	5	–			–			–	
Cejkov	10.60	2.00	5	–			–			–	
Hraň	–			13.51	0.78	1	14.20	0.50	6	–	
Hraň	–			–			**12.45**	**0.40**	2	–	
Hrčeľ	15.70	2.80	3	–			–			–	
Hrčeľ	14.90	2.80	5	–			–			–	
Hrčeľ	13.50	2.50	5	–			–			–	
Malá Bara	16.20	2.00	3	–			14.46	0.95	4	–	
Malá Bara	15.30	2.00	5	–			13.71	0.82	4	–	
Viničky	**12.10**	**0.70**	7	13.52	0.78	1	**11.10**	**0.80**	8	**11.61**	**0.16**
Viničky	**11.40**	**0.50**	5	**12.12**	**0.47**	1	16.53	1.22	4	–	
Viničky	**11.10**	**0.80**	5	**11.19**	**0.53**	1	15.13	0.79	4	–	
Viničky	–			**11.04**	**0.34**	1	14.76	0.90	4	–	
Viničky	–			–			**12.19**	**0.21**	2	–	

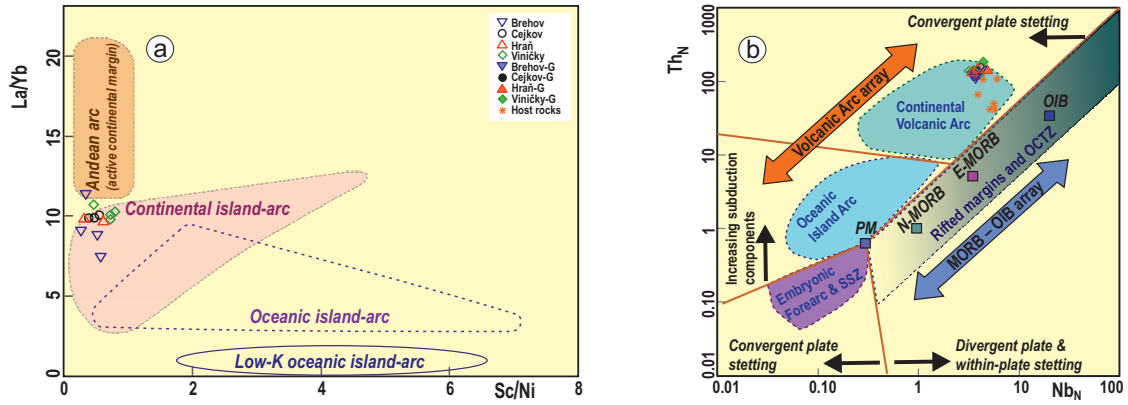

Fig. 8. Tectonic discrimination diagrams for the studied obsidians and their host rocks: **a** — La/Yb versus Sc/Ni diagram (after Bailey 1981); **b** — Th_N vs. Nb_N diagram according Saccani (2015), Nb and Th are normalized to the N-MORB composition (Sun & McDonough 1989). Abbreviations: PM – primitive mantle, MORB – mid-ocean ridge basalts, N-MORB – normal MORB, E-MORB – enriched MORB; OIB – ocean island basalts; SSZ – supra-subduction zone, OCTZ – ocean-continent transition zone.

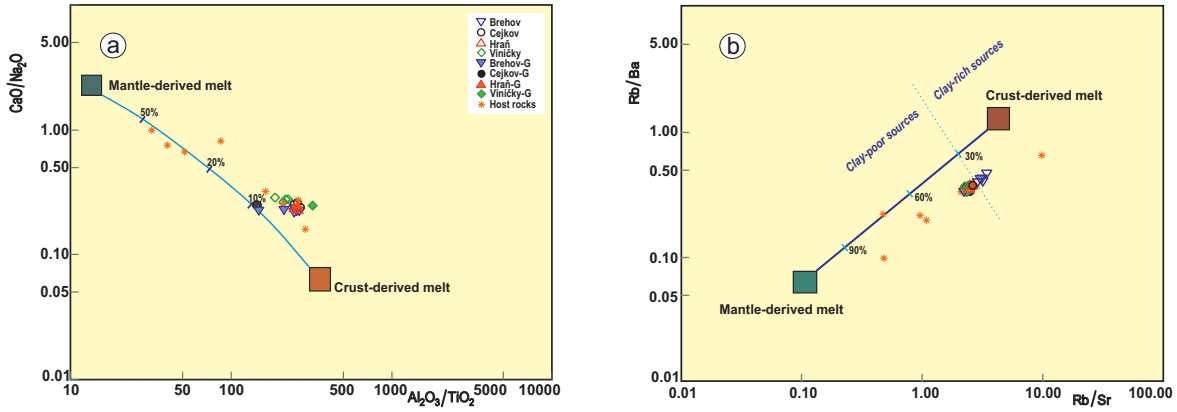

Fig. 9. Binary diagrams used to estimate mixing of mantle (basaltic) and crustal magmatic melts: **a** — CaO/Na_2O vs. Al_2O_3/TiO_2 major elements diagram (all in wt.%); **b** — Rr/Ba vs. Rb/Sr trace elements diagram (all in ppm). Both trajectories indicate dominance of crustal melt (70 ~ 90 %). The compositions of the end members are taken from Sylvester (1998).

dacite host rocks represent typical products of a volcanic arc. They were derived from multi-stage processes in which primary basaltic magma formed due to melting of a lower crustal source at the mantle/crust boundary. Subsequently, melt reservoirs were formed in the middle and upper crust, accompanied by secondary melting of the surrounding rocks, and by recurrent mixing with an ascending lower crustal SCLM influenced melt, and/or repeated assimilation and fractionation. In the Zemplínske vrchy Mts. the result was a chemically variable suite of lithologies ranging from andesite to rhyolites and/or obsidians that formed before 12.0–11.4 Ma. However, nearly identical model of origin was suggested for the host rocks rhyolites and dacites on the basis of their geochemistry by Konečný (2010) and Lexa et al. (2010).

Conclusions

Newly obtained Ar–Ar ages of the Carpathian ***C1*** obsidians from the studied localities, Brehov, Cejkov, and Viničky, define a narrow age interval of 12.07±0.37 to 11.44±0.39 Ma for the younger rhyolitic volcanism unit in the ZVM. A short-time emplacement of ca. 12.0±0.5 Ma suggests that the majority of the ***C1*** obsidian findings come from the Viničky–Borsuk monogenic volcano in the Zemplín volcanic area. The studied ***C1*** obsidians have identical chemical compositions with almost identical physical properties. Geochemically, the ZVM obsidians are acid, fractionated volcanic peraluminous rocks of the high potassium calc-alkaline rhyolite series, with a ferroan character. The Carpathian ***C1*** obsidians and their host rocks represent typical magmatic products of a volcanic arc. They originated through multi-stage magmatic processes of a primary basaltic magma that formed due to melting of lower crustal sources at the mantle/crust border. Subsequent formation of melt reservoirs in the middle and upper crust, accompanied by secondary melting of the surrounding rocks with recurrent addition of an ascending melt, and repeated processes of assimilation and fractionation produced a suite of chemically variable lithology from andesites to rhyolites and obsidians before 12.0–11.4 Ma in the ZVM.

Acknowledgments: MK is greatly appreciated support from the Slovak Research and Development Agency: Grant APVV-0549-07 and APVV-18-0107. Pavel Bačo is thanked for graciously providing a first set of obsidian samples for study. Constructive reviews and valuable comments by Martin Jan Timmerman and Jaroslav Lexa helped to improve the manuscript; Lukáš Krmíček is thanked for editorial handling.

References

Bachmann O. & Bergantz G.W. 2008: Rhyolites and their source mushes across tectonic settings. *Journal of Petrology* 49, 2277–2285. https://doi.org/10.1093/petrology/egn068

Bačo P., Kaminská Ľ., Lexa J., Pécskay Z., Bačová Z. & Konečný V. 2017: Occurrences of Neogene Volcanic Glass in the Eastern Slovakia – Raw Material source for the Stone Industry. *Anthropologie* LV/1–2, 207–230.

Bagdasarjan G.P., Vass D. & Konečný D. 1968: Results of absolute age determination of rocks in the Central and Eastern Slovakia. *Geologica Carpathica* 19, 419–425.

Bagdasarjan G.P., Slávik J. & Vass D. 1971: Chronostratigrafický a biostratigrafický vek niektorých významných neovulkanitov Východného Slovenska [Chronostratigraphic and biostratigraphic age of some important neovolcanics in the Eastern Slovakia]. *Geologické práce, Správy* 58, 87–96 (in Slovak with English summary).

Bailey J.C. 1981: Geochemical criteria for a refined tectonic discrimination of orogenic andesites. *Chemical Geology* 32, 139–154. https://doi.org/10.1016/0009-2541(81)90135-2

Balogh K. & Rakovits Z. 1976: K–Ar ages of Miocene volcanites from NE Hungary. *Annual Report of the Hungarian Geologica Institute* 1974, 471–476.

Balogh K., Pécskay Z., Széky-Fux V. & Gyarmati P. 1983: Chronology of Miocene volcanism in north-east Hungary. In: Proceedings XIIth. Congress CBGA, Bucharest, l49–158.

Baňacký V., Elečko M., Kaličiak M., Straka P., Škvarka L., Šucha P., Vass D., Vozárová A. & Vozár J. 1989: Vysvetlivky ku geolo-

gickej mape južnej časti Východoslovenskej nížiny a Zemplínskych vrchov 1: 50 000 [Explanatory notes to the geological map of the southern part of the East Slovakian Lowlands and the Zemplín Hills in a scale of 1: 50,000]. *Dionýz Štúr Institute of Geology Publisher*, 1–143 (in Slovak with English summary).

Bigazzi G., Màrton P., Norelli P. & Rozložník L. 1990: Fission track dating of Carpathian obsidian and provenance identification. *Nuclear Tracks and Radiation Measurements* 17, 391–399. https://doi.org/10.1016/1359-0189(90)90062-3

Bigazzi G., Biró K.T. & Oddone M. 2000: The Carpathian sources of raw material for obsidian tool-making. (Neutron activation and fission track analyses on the Bodrogkeresztur-Henye Upper Palaeolithic artefacts) In: Dobosi V.T. (Ed.): Bodrogkeresztúr-Henye, NE Hungary, Upper Palaeolithic Site. *Magyar Nemzeti Muzeum*, Budapest, 221–240.

Biró K.T. 2006: Carpathian obsidians: myth and reality. In: Proceedings of the 34th Intern. Symp. on Archaeometry, 3–7 May 2004, Zaragoza, *Institución Fernando el Católico* (C.S.I.C.), 267–278.

Boynton W.V. 1984: Cosmochemistry of the rare earth elements: meteorite studies. In: Henderson P. (Ed.): Developments in geochemistry, Vol. 2. *Elsevier*, 63–114. https://doi.org/10.1016/B978-0-444-42148-7.50008-3

Chappell B.W. & White A.J.R. 1992: I- and S-type granites in the Lachlan Fold Belt. *Transactions of the Royal Society of Edinburgh: Earth Sciences* 83, 1–26.

Cox K.G., Bell J.D. & Pankhurst R.J. 1979: The Interpretation of Igneous Rocks. *George Allen & Unwin*, London, 1–450.

De la Roche H., Leterrier J., Grandclaude P. & Marchal M. 1980: A classification of volcanic and plutonic rocks using R_1–R_2 diagram and major element analyses. Its relationships with current nomenclature. *Chemical Geology* 29, 183–210. https://doi.org/10.1016/0009-2541(80)90020-0

Faryad S.W. & Vozárová A. 1997: Geology and metamorphism of the Zemplinicum basement unit (Western Carpathians). In: Grecula P., Hovorka D. & Putiš M. (Eds.): Geological evolution of the Western Carpathians. *Mineralia Slovaca – Monograph*, Bratislava, 351–358.

Frost B.R., Barnes C.G., Collins W.J., Arculus R.J., Ellis D.J. & Frost C.D. 2001: A geochemical classification for granitic rocks. *Journal of Petrology* 42, 2033–2048. https://doi.org/10.1093/petrology/42.11.2033

Illášová Ľ. & Spišiak J. 2011: Šperkové kamene Slovenska. 1. časť: Prírodné sklá [Gemstones of Slovakia. Part 1: Natural glasses]. *Univerzita Konštantína Filozofa v Nitre*, 1–128 (in Slovak).

Irvine T.N.J. & Baragar W.R.A. 1971: A guide to the chemical classification of the common volcanic rocks. *Canadian Journal of Earth Sciences* 8, 523–548. https://doi.org/10.1139/e71-055

Kaličiak M. & Žec B. 1995: Review of the Neogene volcanism of Eastern Slovakia. *Acta Vulcanologica* 7, 87–95.

Kaminská Ľ. & Ďuďa R. 1985: K otázke významu obsidiánovej suroviny v paleolite Slovenska [Zur Frage der Bedeutung des Obsidianrohstoffes im Paläolithikum der Slowakei]. *Archeologické rozhledy* 37, 121–129 (in Slovak with German summary).

Kobulský J., Žecová K., Gazdačko Ľ., Bačo P., Bačová Z., Maglay J., Petro Ľ. & Šesták P. 2014: Guidebook to Geological–Educational Map of the Zemplínske vrchy Mts. *Dionýz Štúr State Institute of Geology Publisher*, Bratislava, 1–84.

Kohút M., Kollárová V., Mikuš T., Konečný P., Šurka J., Milovská S., Holický I. & Bačo P. 2018: The mineralogy and petrology of the Carpathian obsidians. In: Proceedings of the CEMC-2018, June 26th–30th 2018. Banská Štiavnica, 50–52.

Kohút M., Čižmár E., Dekan J., Drábik M., Hrouda F., Jesenák K., Kliuikov A., Miglierini M., Mikuš T., Milovská S., Šauša O., Šurka J. & Bačo P. 2019:. Physical methods of the Carpathian obsidians study. In: Markó A., Szilágyi K. & Biró K.T. (Eds.): *International Obsidian Conference 2019 Program, Abstracts, Field Guide*; 27–29 May 2019, Sárospatak (Hungary). *Hungarian National Museum*, 37.

Kohút M., Westgate J.A., Pearce N.J. & Bačo P. 2021: The Carpathian obsidians – Contribution to their FT dating and provenance (Zemplín, Slovakia). *Journal of Archaeological Science: Reports* 37, 102861. https://doi.org/10.1016/j.jasrep.2021.102861

Konečný P. 2010: Petrografia a petrológia ryolitových hornín Východného Slovenska [Petrography and petrology of the rhyolite rocks in the Eastern Slovakia]. In: Demko R. (Ed.): Mapy paleovulkanickej rekonštrukcie ryolitových vulkanitov Slovenska a analýza magmatických a hydrotermálnych procesov [The maps of paleovolcanic reconstruction of rhyolite volcanics in Slovakia and an analysis of magmatic and hydrothermal processes]. *Open file report, Archive Geofond*, Bratislava, 397–454 (in Slovak).

Lee J-Y., Marti K., Severinghaus J.P., Kawamura K., Yoo H-S., Lee J.B. & Kim J.S. 2006: A redetermination of the isotopic abundances of atmospheric Ar. *Geochimica et Cosmochimica Acta* 70, 4507–4512. https://doi.org/10.1016/j.gca.2006.06.1563

Lexa J. & Kaličiak M. 2000: Geotectonic aspects of the Neogene volcanism in Eastern Slovakia. *Mineralia Slovaca* 32, 205–210.

Lexa J., Seghedi I., Németh K., Szakács A., Konečný V., Pécskay Z., Fülöp A. & Kovacs M. 2010: Neogene–Quaternary volcanic forms in the Carpathian–Pannonian Region: a review. *Central European Journal of Geosciences* 2, 207–270. https://doi.org/10.2478/v10085-010-0024-5

Ludwig K.R. 2003: User's Manual for ISOPLOT/Ex version 3.0: A geochronological toolkit for Microsoft Excel. *Berkeley Geochronology Center Special Publication* 4, 1–70.

Maniar P.D. & Piccoli P.M. 1989: Tectonic discrimination of granitoids. *Geological society of America Bulletin* 101, 635–643. https://doi.org/10.1130/0016-7606(1989)101<0635:TDOG>2.3.CO;2

Middlemost E.A.K. 1994: Naming material in the magma/igneous rock system. *Earth-Science Reviews* 37, 215–224. https://doi.org/10.1016/0012-8252(94)90029-9

Mielke P. & Winkler H.G.F. 1979: Eine bessere Berechnung der Mesonorm für granitische Gesteine. *Neues Jahrbuch für Mineralogie, Monatshefte* 10, 471–480.

Niggli P. 1923: Gesteins und Mineralprovinzen. *Gebrűder Borntträger*, Berlin, 1–602.

O'Connor J.T. 1965: A classification for Quartz-rich igneous rocks based on feldspar ratios. *U.S. Geological Survey Professional Paper* 525-B, B79–B84.

Oddone M., Marton P., Bigazzi G. & Biró K. 1999: Chemical characterisations of Carpathian obsidian sources by instrumental and epithermal neutron activation analysis. *Journal of Radioanalytical and Nuclear Chemistry* 240, 147–153.

Pearce J.A. 1982: Trace element characteristics of lavas from destructive plate boundaries. In: Thorpe R.S. (Ed.): Andesites – Orogenic Andesites and related rocks, *John Wiley & Sons*, Chichester, 525–548.

Pearce J.A. 1996: A user's guide to basalt discrimination diagrams. In: Wyman D.A. (Ed.): Trace Element Geochemistry of Volcanic Rocks: Applications for Massive Sulphide Exploration. *Geological Association of Canada, Short Course Notes* 12, 79–113.

Peccerillo A. & Taylor S.R. 1976: Geochemistry of Eocene calc-alkaline volcanic rocks from the Kastamonu area, Northern Turkey. *Contribution to Mineralogy and Petrology* 58, 63–81. https://doi.org/10.1007/BF00384745

Pécskay Z., Balogh K., Széky-Fux V. & Gyarmati P. 1986: Geochronological investigations on the Neogene volcanism of the Tokaj Mountains. *Geologica Carpathica* 37, 635–655.

Pécskay Z., Lexa J., Szakács A., Seghedi I., Balogh K., Konečný V., Zelenka T., Kovacs M., Póka T., Fülöp A., Márton E., Panaiotu C. & Cvetković V. 2006: Geochronology of Neogene magma-

tism in the Carpathian arc and intra-Carpathian area. *Geologica Carpathica* 57, 511–530.

Plank T. & Langmuir C.H. 1998: The chemical composition of subducting sediment and its consequences for the crust and mantle. *Chemical Geology* 145, 325–394. https://doi.org/10.1016/S0009-2541(97)00150-2

Renne P.R., Blaco G., Ludwig K.R., Mundil R. & Min K. 2011: Response to the comment by W.H. Schwarz et al. on "Joint determination of ^{40}K decay constants and ^{40}Ar*/^{40}K for the Fish Canyon sanidine standard, and improved accuracy for ^{40}Ar/^{39}Ar geochronology" by P.R. Renne et al. (2010). *Geochimica et Cosmochimica Acta* 75, 5097–5100. https://doi.org/10.1016/j.gca.2011.06.021

Repčok I. 1977: Stopy delenia uránu a možnosti ich využitia pre datovanie na príklade vulkanických skiel [The Uranium fission tracks and the possibility of their use for dating of the volcanic glasses]. *Západné Karpaty, séria mineralógia, petrografia, geochémia, ložiská* 3, 175–196 (in Slovak with English summary).

Repčok I., Kaličiak M. & Bacsó Z. 1988: Vek niektorých vulkanitov východného Slovenska určený metódou stop po štiepení uránu [The Age of some volcanics in eastern Slovakia determined by the Uranium fission tracks method]. *Západné Karpaty, séria mineralógia, petrografia, geochémia, ložiská* 11, 75–88 (in Slovak with English summary).

Rosania C.N., Boulanger M.T., Biró K.T., Ryzhov S., Trnka G. & Glascock M.D. 2008: Revisiting Carpathian obsidian. *Antiquity* 82, 318–320.

Rózsa P., Szöőr G., Elekes Z., Gratuze B., Uzonyi I. & Kiss Á.Z. 2006: Comparative geochemical studies of obsidian samples from various localities. *Acta Geologica Hungarica* 49, 73–87. https://doi.org/10.1556/ageol.49.2006.1.5

Saccani E. 2015: A new method of discriminating different types of post-Archean ophiolitic basalts and their tectonic significance using Th-Nb and Ce-Dy-Yb systematics. *Geoscience Frontiers* 6, 481–501. https://doi.org/10.1016/j.gsf.2014.03.006

Salters V.J., Hart S.R. & Pantó G. 1988: Origin of Late Cenozoic Volcanic Rocks of the Carpathian Arc, Hungary. In: Royden L.H. & Horvath F. (Eds.): The Pannonian Basin: A Study in Basin Evolution. *AAPG Memoir* 45, 279–292.

Seghedi I. & Downes H. 2011: Geochemistry and tectonic development of Cenozoic magmatism in the Carpathian–Pannonian region. *Gondwana Research* 20, 655–672. https://doi.org/10.1016/j.gr.2011.06.009

Slávik J. 1968: Chronology and Tectonic Background of the Neogene Volcanism in East Slovakia. *Geologické práce, Správy* 44, 199–214.

Streckeisen A. 1976: Classification of the common igneous rocks by means of their chemical composition: a provisional attempt JV. *Neues Jahrbuch für Mineralogie, Monatshefte* 1, 1–15.

Streckeisen A. & Le Maitre R.W. 1979: A chemical approximation to the modal QAPF classification of the igneous rocks. *Neues Jahrbuch für Mineralogie, Abhandlungen* 136, 169–206.

Sun S.S. & McDonough W.F. 1989: Chemical and isotopic systematics of oceanic basalts: implications for mantle composition and processes. *Geological Society, London, Special Publications* 42, 313–345. https://doi.org/10.1144/GSL.SP.1989.042.01.19

Sylvester P.J. 1998: Post-collisional strongly peraluminous granites. *Lithos* 45, 29–44. https://doi.org/10.1016/S0024-4937(98)00024-3

Szepesi J., Lukács R., Soós I., Benkó Z., Pécskay Z., Ésik Z., Kozák M., Di Capua A., Groppelli G., Norini G., Sulpizio R. & Harangi S. 2019: Telkibánya lava domes: Lithofacies architecture of a Miocene rhyolite field (Tokaj Mountains, Carpathian-Pannonian region, Hungary). *Journal of Volcanology and Geothermal Research* 385, 179–197. https://doi.org/10.1016/j.jvolgeores.2019.07.002

Šalát J. & Ončáková P. 1964: Perlity, ich výskyt, petrochémia a praktické použitie [Perlites, their occurrence, petrochemistry and practical use]. *Veda Publishing House of the Slovak Academy of Sciences*, Bratislava, 1–147 (in Slovak).

Taylor S.R. & McLennan S.M. 2001: Chemical composition and element distribution in the Earth's crust. *Encyclopedia of physical science and technology* 312, 697–719.

Tsoň O.V. & Slávik J. 1971: Vek ryolitov Zemplínskeho ostrova [Age of the Zemplín island rhyolites]. *Geologické práce, Správy* 50, 215–216 (in Slovak).

Vass D., Bagdasarjan G.P. & Konečný V. 1971: Determination of the absolute age of the West Carpathian Miocene. *Földtani Közlemény* 101, 321–327.

Vass D., Tözser J., Bagdasarjan G.P., Kaličiak M., Orlický O. & Ďurica D. 1978: Chronológia vulkanických udalostí na východnom Slovensku vo svelte izotopických a paleomagnetických výskumov [Chronology of volcanic events in Eastern Slovakia on the basis of isotopical–paleomagnetical researches]. *Geologické práce, Správy* 71, 77–88 (in Slovak with English summary).

Vass D., Bañacký V. & Kaličiak M. 1991: Odkrytá geologická mapa Východoslovenskej nížiny 1:100 000 [Exposed geological map of the East Slovakian Basin on a scale 1:100,000]. *Dionýz Štúr Institute of Geology Publisher*, Bratislava.

Williams-Thorpe O., Warren S.E. & Nandris J.G. 1984: The distribution and provenance of archaeological obsidian in Central and Eastern Europe. *Journal of Archaeological Science* 11, 183–212. https://doi.org/10.1016/0305-4403(84)90001-3

Appendix

GPS localization of studied samples:

Sample	Locality	Latitude (°N)	Longitude (°E)
Br-1	Brehov–1	48°29'40.70"	21°47'50.10"
Br-2	Brehov–2	48°29'42.40"	21°48'15.00"
Ce-1	Cejkov–1	48°28'14.60"	21°47'12.50"
Hr-1	Hraň–1	48°31'08.60"	21°47'14.60"
V-1	Viničky–1	48°24'04.90"	21°44'16.70"

Supplementary material

Supplementary Table S1 is available online at http://geologicacarpathica.com/data/files/supplements/GC-72-4-Kohut_TableS1.xlsx.

Supplementary Table S1: $^{40}Ar/^{39}Ar$ spot ablation ages of dated Carpathian obsidians from the Zemplín area, Slovakia. J values used: Br-1=0.000336082; Br-2=0.000337465; Ce-1=0.0003406696 and V-1=0.000344851.

Run No	Type	^{40}Ar	±1 s	^{39}Ar	±1 s	^{38}Ar	±1 s	^{37}Ar	±1 s	^{36}Ar	±1 s	$^{40}Ar^*/^{39}Ar$	± 1 s	Age	± 1 s	±1s (no J error)	39/40	±1 s	36/40	±1 s	37/39	±1 s	38/39	±1 s
W17A56471	Br-1 gl	0.23917	0.00230	0.01239	0.00040	0.00020	0.00007	0.00154	0.00010	0.00010	0.00003	16.852	0.931	10.29	0.57	0.567	0.0518	0.0017	0.0004	0.0001	0.1243	0.0091	0.0163	0.0058
W17A56539	Br-1 gl	0.11177	0.00118	0.00564	0.00022	0.00011	0.00005	0.00058	0.00012	0.00005	0.00004	17.007	2.184	10.38	1.33	1.330	0.0504	0.0021	0.0005	0.0003	0.1031	0.0210	0.0199	0.0092
W17A56457	Br-1 gl	0.13424	0.00258	0.00651	0.00028	0.00011	0.00007	0.00042	0.00010	0.00007	0.00004	17.313	1.928	10.57	1.17	1.173	0.0485	0.0023	0.0005	0.0003	0.0651	0.0158	0.0169	0.0110
W17A56462	Br-1 gl	0.25546	0.00327	0.01282	0.00032	0.00015	0.00007	0.00105	0.00010	0.00011	0.00003	17.329	0.869	10.58	0.53	0.529	0.0502	0.0014	0.0004	0.0001	0.0820	0.0082	0.0118	0.0056
W17A56469	Br-1 gl	0.20847	0.00256	0.01034	0.00041	0.00018	0.00009	0.00091	0.00010	0.00008	0.00003	17.806	1.153	10.87	0.70	0.702	0.0496	0.0020	0.0004	0.0001	0.0881	0.0104	0.0176	0.0087
W17A56465	Br-1 gl	0.17910	0.00273	0.00818	0.00030	0.00010	0.00007	0.00091	0.00010	0.00010	0.00005	18.187	1.842	11.10	1.12	1.121	0.0457	0.0018	0.0006	0.0003	0.1112	0.0131	0.0122	0.0088
W17A56460	Br-1 gl	0.24885	0.00332	0.01226	0.00044	0.00014	0.00006	0.00137	0.00010	0.00007	0.00004	18.555	1.166	11.33	0.71	0.709	0.0493	0.0019	0.0003	0.0002	0.1120	0.0092	0.0115	0.0045
W17A56459	Br-1 gl	0.20553	0.00348	0.01051	0.00036	0.00015	0.00006	0.00080	0.00010	0.00003	0.00004	18.648	1.290	11.38	0.79	0.785	0.0511	0.0019	0.0002	0.0002	0.0761	0.0100	0.0144	0.0053
W17A56540	Br-1 gl	0.11964	0.00144	0.00602	0.00029	0.00016	0.00004	0.00025	0.00012	0.00002	0.00003	18.717	1.847	11.42	1.12	1.124	0.0503	0.0025	0.0002	0.0003	0.0418	0.0194	0.0271	0.0074
W17A56472	Br-1 gl	0.23371	0.00290	0.01116	0.00031	0.00015	0.00006	0.00111	0.00010	0.00007	0.00004	19.017	1.169	11.61	0.71	0.711	0.0478	0.0014	0.0003	0.0002	0.0994	0.0095	0.0135	0.0057
W17A56546	Br-1 gl	0.10541	0.00205	0.00502	0.00026	0.00007	0.00005	0.00039	0.00012	0.00003	0.00004	19.028	2.562	11.61	1.56	1.558	0.0476	0.0027	0.0003	0.0004	0.0774	0.0235	0.0142	0.0103
W17A56468	Br-1 gl	0.32911	0.00368	0.01600	0.00038	0.00022	0.00008	0.00150	0.00010	0.00005	0.00004	19.607	0.874	11.96	0.53	0.532	0.0486	0.0013	0.0002	0.0001	0.0939	0.0067	0.0139	0.0050
W17A56474	Br-1 gl	0.11682	0.00261	0.00563	0.00026	0.00005	0.00006	0.00062	0.00010	0.00002	0.00004	19.609	2.251	11.97	1.37	1.369	0.0482	0.0025	0.0002	0.0003	0.1110	0.0189	0.0086	0.0112
W17A56466	Br-1 gl	0.18191	0.00281	0.00888	0.00022	0.00017	0.00008	0.00091	0.00010	0.00002	0.00005	19.754	1.660	12.05	1.01	1.009	0.0488	0.0014	0.0001	0.0003	0.1024	0.0117	0.0193	0.0091
W17A56545	Br-1 gl	0.10297	0.00219	0.00512	0.00031	0.00002	0.00006	0.00029	0.00012	-0.00001	0.00003	20.497	2.269	12.51	1.38	1.379	0.0497	0.0031	-0.0001	-0.0003	0.0568	0.0229	0.0039	0.0117
W17A56542	Br-1 gl	0.15037	0.00163	0.00659	0.00021	0.00009	0.00005	0.00101	0.00012	0.00004	0.00004	20.871	1.910	12.73	1.16	1.161	0.0438	0.0015	0.0003	0.0003	0.1532	0.0183	0.0139	0.0078
W17A56463	Br-1 gl	0.19671	0.00275	0.00857	0.00034	0.00010	0.00006	0.00085	0.00010	0.00005	0.00003	21.149	1.387	12.90	0.84	0.843	0.0436	0.0018	0.0003	0.0002	0.0997	0.0125	0.0116	0.0074
W17A56543	Br-1 gl	0.10424	0.00139	0.00495	0.00023	0.00005	0.00006	0.00087	0.00012	-0.00001	0.00003	21.494	2.200	13.11	1.34	1.337	0.0474	0.0023	-0.0001	-0.0003	0.1767	0.0249	0.0102	0.0121
W17A56475	Br-1 gl	0.16471	0.00261	0.00756	0.00035	0.00016	0.00004	0.00077	0.00010	0.00000	0.00003	21.724	1.602	13.25	0.97	0.974	0.0459	0.0022	0.0000	0.0002	0.1017	0.0143	0.0213	0.0052
W17A56533	Br-2 gl	0.04511	0.00320	0.00245	0.00020	-0.00003	0.00006	0.00013	0.00011	0.00001	0.00003	17.199	4.407	10.54	2.69	2.694	0.0543	0.0059	0.0002	0.0007	0.0527	0.0455	-0.0131	-0.024
W17A56511	Br-2 gl	0.09035	0.00186	0.00481	0.00037	0.00005	0.00004	0.00039	0.00013	0.00001	0.00003	17.894	2.143	10.97	1.31	1.310	0.0533	0.0043	0.0002	0.0003	0.0818	0.0277	0.0098	0.0092
W17A56507	Br-2 gl	0.06113	0.00220	0.00335	0.00024	0.00001	0.00005	0.00032	0.00013	0.00000	0.00003	17.901	2.714	10.97	1.66	1.659	0.0547	0.0045	0.0001	0.0004	0.0948	0.0394	0.0019	0.0155
W17A56531	Br-2 gl	0.09376	0.00306	0.00507	0.00020	0.00003	0.00006	0.00028	0.00011	-0.00002	0.00003	19.657	2.153	12.04	1.31	1.315	0.0541	0.0028	-0.0002	-0.0003	0.0559	0.0220	0.0058	0.0117
W17A56508	Br-2 gl	0.07608	0.00201	0.00383	0.00022	0.00003	0.00004	0.00030	0.00013	-0.00001	0.00003	20.311	2.384	12.44	1.46	1.456	0.0504	0.0032	-0.0001	-0.0003	0.0779	0.0342	0.0070	0.0115
W17A56510	Br-2 gl	0.09415	0.00232	0.00464	0.00027	0.00007	0.00005	0.00030	0.00013	-0.00001	0.00003	20.677	2.555	12.67	1.56	1.560	0.0493	0.0031	-0.0001	-0.0004	0.0644	0.0282	0.0146	0.0112
W17A56513	Br-2 gl	0.10583	0.00242	0.00539	0.00025	0.00008	0.00005	0.00041	0.00013	-0.00005	0.00003	22.167	1.817	13.58	1.11	1.109	0.0510	0.0027	-0.0004	-0.0002	0.0766	0.0244	0.0144	0.0096
W17A56514	Br-2 gl	0.09024	0.00183	0.00436	0.00029	0.00010	0.00004	0.00047	0.00013	-0.00004	0.00003	23.161	2.383	14.18	1.45	1.453	0.0483	0.0034	-0.0004	-0.0003	0.1080	0.0307	0.0225	0.0102
W17A56529	Br-2 bt	0.09563	0.00329	0.00513	0.00029	0.00008	0.00007	0.00044	0.00011	0.00002	0.00003	17.497	2.226	10.72	1.36	1.361	0.0536	0.0035	0.0002	0.0003	0.0855	0.0221	0.0157	0.0133
W17A56532	Br-2 bt	0.07587	0.00342	0.00433	0.00023	0.00003	0.00006	0.00026	0.00011	-0.00001	0.00004	18.213	2.993	11.16	1.83	1.829	0.0571	0.0040	-0.0001	-0.0005	0.0611	0.0258	0.0067	0.0137
W17A56501	Br-2 bt	0.09866	0.00186	0.00508	0.00017	0.00007	0.00004	0.00028	0.00013	0.00001	0.00003	18.581	1.669	11.39	1.02	1.020	0.0515	0.0020	0.0001	0.0003	0.0548	0.0255	0.0133	0.0087
W17A56505	Br-2 bt	0.10823	0.00203	0.00588	0.00037	0.00008	0.00004	0.00072	0.00013	-0.00002	0.00003	19.224	1.816	11.78	1.11	1.109	0.0543	0.0036	-0.0001	-0.0002	0.1219	0.0234	0.0132	0.0076
W17A56504	Br-2 bt	0.17321	0.00258	0.00853	0.00033	0.00010	0.00006	0.00093	0.00013	0.00002	0.00003	19.460	1.213	11.92	0.74	0.741	0.0493	0.0021	0.0001	0.0001	0.1084	0.0158	0.0115	0.0071
W17A56499	Br-2 bt	0.08936	0.00213	0.00478	0.00033	0.00001	0.00004	0.00039	0.00013	-0.00002	0.00003	19.675	2.151	12.06	1.31	1.314	0.0535	0.0039	-0.0002	-0.0003	0.0820	0.0276	0.0013	0.0079
W17A56502	Br-2 bt	0.08137	0.00179	0.00415	0.00023	0.00003	0.00006	0.00032	0.00013	-0.00003	0.00003	21.457	2.763	13.14	1.69	1.686	0.0510	0.0031	-0.0003	-0.0004	0.0763	0.0315	0.0064	0.0145
W17A56528	Br-2 bt	0.06575	0.00337	0.00314	0.00023	0.00002	0.00004	0.00030	0.00011	-0.00002	0.00003	22.833	3.669	13.98	2.24	2.238	0.0478	0.0042	-0.0003	-0.0005	0.0964	0.0360	0.0061	0.0115
W17A38888	Ce-1 gl	0.05997	0.00091	0.00335	0.00005	0.00002	0.00002	0.00010	0.00112	0.00000	0.00001	18.119	1.303	11.13	0.80	0.798	0.0559	0.0012	0.0000	-0.0002	0.0307	0.3351	0.0072	0.0063
W17A38892	Ce-1 gl	0.08734	0.00099	0.00468	0.00005	0.00005	0.00002	-0.00155	0.00112	0.00001	0.00001	18.171	0.938	11.16	0.57	0.574	0.0535	0.0009	0.0001	0.0002	-0.3306	-0.240	0.0117	0.0045
W17A38889	Ce-1 gl	0.05019	0.00090	0.00262	0.00009	0.00005	0.00001	0.00010	0.00112	0.00001	0.00001	18.328	1.743	11.26	1.07	1.067	0.0521	0.0020	0.0001	0.0003	0.0394	0.4293	0.0210	0.0044
W17A38891	Ce-1 gl	0.06874	0.00094	0.00371	0.00010	0.00007	0.00002	0.00093	0.00112	0.00000	0.00001	18.736	1.253	11.51	0.77	0.767	0.0540	0.0016	0.0000	-0.0002	0.2498	0.3028	0.0175	0.0057
W17A38895	Ce-1 gl	0.09044	0.00094	0.00445	0.00006	0.00009	0.00002	0.00010	0.00113	0.00002	0.00001	19.159	0.996	11.76	0.61	0.609	0.0492	0.0009	0.0002	0.0002	0.0232	0.2532	0.0192	0.0047
W17A38894	Ce-1 gl	0.06681	0.00101	0.00347	0.00005	0.00005	0.00002	0.00010	0.00113	0.00000	0.00001	19.500	1.272	11.97	0.78	0.778	0.0519	0.0011	0.0000	-0.0002	0.0298	0.3249	0.0159	0.0061
W17A38898	Ce-1 gl	0.32032	0.00127	0.01533	0.00021	0.00025	0.00002	0.00176	0.00113	0.00004	0.00001	20.170	0.396	12.38	0.24	0.242	0.0479	0.0007	0.0001	0.0000	0.1146	0.0735	0.0162	0.0014
W17A38900	Ce-1 gl	0.07333	0.00088	0.00363	0.00006	0.00004	0.00002	-0.00155	0.00113	0.00000	0.00001	20.363	1.221	12.50	0.75	0.747	0.0495	0.0010	0.0000	-0.0002	-0.4270	-0.311	0.0123	0.0058
W17A38901	Ce-1 gl	0.07111	0.00098	0.00339	0.00008	0.00005	0.00002	0.00507	0.00113	0.00001	0.00001	20.437	1.351	12.55	0.83	0.826	0.0477	0.0013	0.0001	0.0002	1.4950	0.3347	0.0162	0.0062
W17A38706	Ce-1 gl	0.13996	0.00237	0.00714	0.00034	0.00006	0.00013	-0.00331	0.00899	-0.00002	0.00008	20.438	3.334	12.55	2.04	2.039	0.0510	0.0026	-0.0001	-0.0005	-0.4641	-1.259	0.0077	0.0186
W17A38708	Ce-1 bt	0.09118	0.00236	0.00484	0.00035	0.00000	0.00013	-0.00523	0.00899	-0.00004	0.00007	21.293	4.819	13.07	2.95	2.948	0.0531	0.0040	-0.0004	-0.0008	-1.0794	-1.858	0.0008	0.0275
W17A38715	Ce-1 bt	0.05974	0.00234	0.00280	0.00034	-0.00004	0.00013	-0.00524	0.00901	-0.00003	0.00007	24.492	8.432	15.03	5.15	5.151	0.0470	0.0060	-0.0005	-0.0012	-1.8670	-3.219	-0.0131	-0.047
W17A38709	Ce-1 bt	0.04051	0.00236	0.00204	0.00034	-0.00006	0.00013	-0.00587	0.00899	-0.00004	0.00007	25.723	11.66	15.78	7.12	7.119	0.0503	0.0088	-0.0010	-0.0018	-2.8769	-4.436	-0.0281	-0.065
W17A38718	Ce-1 bt	0.06859	0.00234	0.00308	0.00034	-0.00005	0.00013	-0.00780	0.00901	-0.00004	0.00007	26.111	7.732	16.01	4.72	4.721	0.0450	0.0052	-0.0006	-0.0011	-2.5279	-2.936	-0.0152	-0.043
W17A38717	Ce-1 bt	0.04523	0.00235	0.00195	0.00034	-0.00006	0.00013	-0.00588	0.00901	-0.00003	0.00007	27.845	12.37	17.07	7.55	7.549	0.0430	0.0078	-0.0007	-0.0016	-3.0204	-4.661	-0.0294	-0.068
W17A38931	V1 gl	0.05535	0.00096	0.00287	0.00007	0.00003	0.00001	-0.00049	0.00136	0.00002	0.00001	16.922	1.379	10.50	0.85	0.853	0.0518	0.0015	0.0004	0.0002	-0.1710	-0.476	0.0090	0.0046
W17A38906	V1 gl	0.05098	0.00051	0.00275	0.00010	0.00003	0.00001	-0.00019	0.00162	0.00001	0.00001	17.473	1.645	10.84	1.02	1.018	0.0539	0.0021	0.0002	0.0003	-0.0680	-0.591	0.0112	0.0048
W17A38928	V1 gl	0.05157	0.00096	0.00280	0.00006	0.00004	0.00002	0.00037	0.00136	0.00000	0.00001	18.107	1.404	11.23	0.87	0.869	0.0543	0.0016	0.0001	0.0002	0.1310	0.4864	0.0128	0.0079
W17A38916	V1 gl	0.05066	0.00056	0.00263	0.00007	0.00003	0.00002	0.00150	0.00163	0.00001	0.00001	18.168	1.654	11.27	1.02	1.023	0.0519	0.0016	0.0002	0.0003	0.5693	0.6185	0.0117	0.0084
W17A38935	V1 gl	0.11849	0.00112	0.00645	0.00009	0.00011	0.00002	0.00123	0.00137	0.00000	0.00001	18.240	0.639	11.32	0.40	0.395	0.0545	0.0009	0.0000	0.0001	0.1900	0.2116	0.0166	0.0034
W17A38910	V1 gl	0.09867	0.00092	0.00537	0.00011	0.00010	0.00002	0.00149	0.00162	0.00000	0.00001	18.387	0.875	11.41	0.54	0.541	0.0545	0.0013	0.0000	-0.0001	0.2782	0.3022	0.0190	0.0041
W17A38932	V1 gl	0.07542	0.00097	0.00389	0.00009	0.00005	0.00002	0.00037	0.00136	0.00001	0.00001	18.413	1.053	11.42	0.65	0.651	0.0516	0.0013	0.0002	0.0002	0.0945	0.3509	0.0119	0.0057
W17A38907	V1 gl	0.08771	0.00067	0.00471	0.00009	0.00007	0.00002	0.00149	0.00162	0.00000	0.00001	18.645	0.958	11.57	0.59	0.592	0.0537	0.0011	0.0000	-0.0002	0.3171	0.3444	0.0152	0.0047
W17A38937	V1 gl	0.14660	0.00108	0.00660	0.00014	0.00009	0.00002	-0.00135	0.00137	0.00007	0.00001	18.896	0.706	11.72	0.44	0.437	0.0450	0.0010	0.0005	0.0001	-0.2045	-0.207	0.0132	0.0034
W17A38938	V1 gl	0.05131	0.00092	0.00268	0.00010	0.00004	0.00002	0.00209	0.00137	0.00000	0.00001	18.908	1.557	11.73	0.96	0.963	0.0522	0.0021	0.0000	0.0002	0.7797	0.5115	0.0134	0.0083
W17A38929	V1 gl	0.07948	0.00101	0.00399	0.00009	0.00007	0.00002	-0.00135	0.00136	0.00001	0.00001	18.914	1.032	11.73	0.64	0.638	0.0502	0.0013	0.0002	0.0002	-0.3373	-0.342	0.0167	0.0055
W17A38912	V1 gl	0.06209	0.00056	0.00343	0.00008	0.00004	0.00001	-0.00019	0.00162	-0.00001	0.00001	18.976	1.293	11.77	0.80	0.800	0.0552	0.0014	-0.0002	-0.0002	-0.0545	-0.474	0.0119	0.0039
W17A38921	V1 gl	0.07910	0.00061	0.00417	0.00006	0.00005	0.00002	0.00150	0.00163	0.00000	0.00001	18.986	1.035	11.78	0.64	0.640	0.0527	0.0009	0.0000	-0.0002	0.3595	0.3905	0.0122	0.0053
W17A38922	V1 gl	0.06635	0.00058	0.00333	0.00007	0.00006	0.00001	0.00150	0.00163	0.00001	0.00001	19.039	1.311	11.81	0.81	0.811	0.0503	0.0012	0.0001	0.0002	0.4499	0.4888	0.0184	0.0040
W17A38909	V1 gl	0.05290	0.00056	0.00278	0.00005	0.00001	0.00002	-0.00019	0.00162	0.00000	0.00001	19.044	1.535	11.81	0.95	0.949	0.0525	0.0011	0.0000	0.0003	-0.0673	-0.585	0.0037	0.0080
W17A38919	V1 gl	0.05934	0.00066	0.00287	0.00009	0.00006	0.00001	-0.00019	0.00163	0.00001	0.00001	19.631	1.584	12.18	0.98	0.979	0.0484	0.0017	0.0002	0.0002	-0.0653	-0.567	0.0214	0.0047
W17A38918	V1 gl	0.07424	0.00078	0.00378	0.00006	0.00005	0.00001	0.00066	0.00163	0.00000	0.00001	19.655	1.152	12.19	0.71	0.712	0.0509	0.0010	0.0000	-0.0002	0.1735	0.4306	0.0135	0.0035
W17A38913	V1 gl	0.05721	0.00062	0.00286	0.00007	0.00003	0.00001	-0.00019	0.00163	0.00000	0.00001	20.001	1.539	12.40	0.95	0.951	0.0500	0.0014	0.0000	0.0002	-0.0654	-0.568	0.0107	0.0046
W17A38934	V1 gl	0.07997	0.00093	0.00403	0.00007	0.00005	0.00001	-0.00135	0.00137	-0.00001	0.00001	20.321	0.997	12.60	0.62	0.616	0.0505	0.0011	-0.0001	-0.0002	-0.3343	-0.338	0.0114	0.0033
W17A38915	V1 gl	0.05796	0.00054	0.00287	0.00007	0.00004	0.00001	0.00066	0.00163	-0.00001	0.00001	21.258	1.541	13.18	0.95	0.952	0.0495	0.0013	-0.0002	-0.0002	0.2283	0.5668	0.0142	0.0046